Femtosecond quantum control of molecular dynamics in the condensed phase

Patrick Nuernberger, Gerhard Vogt, Tobias Brixner and Gustav Gerber*

Received 22nd December 2006, Accepted 12th February 2007
First published as an Advance Article on the web 13th March 2007
DOI: 10.1039/b618760a

We review the progress in controlling quantum dynamical processes in the condensed phase with femtosecond laser pulses. Due to its high particle density the condensed phase has both high relevance and appeal for chemical synthesis. Thus, in recent years different methods have been developed to manipulate the dynamics of condensed-phase systems by changing one or multiple laser pulse parameters. Single-parameter control is often achieved by variation of the excitation pulse's wavelength, its linear chirp or its temporal subpulse separation in case of pulse sequences. Multiparameter control schemes are more flexible and provide a much larger parameter space for an optimal solution. This is realized in adaptive femtosecond quantum control, in which the optimal solution is iteratively obtained through the combination of an experimental feedback signal and an automated learning algorithm. Several experiments are presented that illustrate the different control concepts and highlight their broad applicability. These fascinating achievements show the continuous progress on the way towards the control of complex quantum reactions in the condensed phase.

I. Introduction

Optical time-resolved spectroscopy and frequency-resolved techniques have revealed the characteristic dynamical behavior of various quantum mechanical systems. We nowadays have a good knowledge, for example, of the early-time and long-time electronic and rovibrational dynamics in many molecules ranging from diatomics all the way to biomolecular complexes. The growing understanding of these quantum processes has opened up the perspective for not only observing but in fact also controlling their dynamical behavior. In the case of manipulating chemical reactions, for example, the goal could be to generate certain chemical products with high efficiency while at the same time reducing unwanted side products. This concept of steering the outcome of quantum time evolution into certain directions by application of suitable optical fields is in general called ''quantum control'' or ''coherent control''. Of course this principle is not limited to molecules but can also be applied to other quantum systems.

There are a number of different theoretical schemes and experimental scenarios that have been developed over the years predicting and illustrating how specific properties of laser radiation can be exploited and manipulated in order to achieve certain quantum control targets. One of the early approaches was to make use of the high monochromaticity and tunability of narrow-band lasers for selective bond breakage. The intuitive concept was to adjust the irradiation wavelength to the local vibrational frequency of a particular bond such that high intensity input would lead to selective dissociation of the excited bond.[1,2]

Universität Würzburg, Physikalisches Institut, Am Hubland, 97074 Würzburg, Germany. E-mail: gerber@physik.uni-wuerzburg.de

Unfortunately, in most cases the ultrafast intramolecular vibrational redistribution (IVR) of the deposited energy prevents the breaking of the desired bond, unless it is the weakest.[3–7] This problem already occurs for isolated molecules in the gas phase. In the condensed phase, the coupling to the environment (*e.g.*, solvent molecules) provides an additional channel for energy redistribution. Hence the problem of quantum control is in general complicated, and appropriate control concepts have to be developed.

Although this review is about quantum control in the condensed phase, we will not discuss optimization of second-harmonic generation (SHG) in nonlinear crystals[8–19] or some other multiparameter demonstrations related to solid-state physics, *e.g.* applications to semiconductors or quantum dots,[20–27] including the experiment by Nelson and coworkers,[28] who employed pulse shaping techniques to spatiotemporally control lattice vibrational waves. Instead, we will deal with control problems in which photoinduced quantum dynamical processes (such as selective photoexcitation, wave packet propagation, or ultrafast chemical reactions) of condensed phase molecular systems are in the foreground.

A. Quantum control concepts

In the 1980s, several quantum control concepts were suggested and later verified experimentally. One of these is the scheme proposed by Brumer and Shapiro in 1986,[29,30] first demonstrated in 1990.[31] It exploits the interference between different pathways that connect initial and final states of the investigated quantum system. The population in the final state can be modulated *via* constructive or destructive interference by modifying the relative phase between the two (continuous-wave) excitation lasers that correspond to different pathways.

Another control concept was proposed by Tannor, Kosloff and Rice[32–34] in 1985 and is commonly explained in the time domain. Here a vibrational wave packet is induced by an ultrashort excitation laser pulse on an excited potential energy surface (PES). When, after free evolution of the system, the molecule has reached a configuration that is favorable for a certain reaction outcome, a second ultrashort laser pulse transfers the population to the product state. Control is possible by adjusting the time delay between excitation and dump laser pulse (for details, see section IIIC). This concept has been first demonstrated in the early 1990s by the groups of Gerber[35–37] and Zewail.[38]

In a further control scheme approach, population transfer in atoms and molecules is implemented by adiabatic passage techniques.[39,40] The system under study is initially in a discrete state when an electric field is applied that is specially suited to transferring the population into a desired target state. The first laser-induced adiabatic rapid passage (ARP) was demonstrated by Loy in 1974[41] with a (quasi-)monochromatic microsecond laser source and a sweeped dc Stark field in order to facilitate a shift of the transition through the resonance. The availability of broadband femtosecond lasers facilitated such a shift by adequately chirping the laser pulse, experimentally realized in 1992.[42,43] In stimulated Raman adiabatic passage (STIRAP), first demonstrated in 1988,[44] two laser pulses are applied to a Λ-type three-level system to achieve a complete population transfer between the two lower levels *via* the intermediate upper level. The two pulses can either be realized by two continuous-wave (cw) laser beams that are spatially displaced but overlap partially (so that for particles crossing the laser beams a sequence of two ''pulsed'' electric fields is mimicked), or by two pulsed laser beams that coincide spatially but have an appropriate time delay.[39,40] If adiabatic conditions are fulfilled and the two pulses' temporal overlap is sufficient, complete population transfer can be achieved with counter-intuitive instead of intuitive pulse ordering. This means that the laser beam coupling the intermediate to the final state precedes the one coupling the initially populated state to the intermediate level. As no population is present in the intermediate level throughout the experiment, unwanted properties of this state, *e.g.* radiative decay, are eluded.

It was suggested by Tannor and Rice[32] that more general control possibilities would arise with complex electric field shapes that are specifically adjusted to the dynamics of the quantum system. This concept of complex laser field shapes was also developed in the context of optimal control theory by Rabitz and coworkers,[45,46] Kosloff and coworkers,[47] Paramonov, Manz and coworkers,[48,49] Fujimura and coworkers,[50] and other groups. The idea was that an optimal ''guidance'' of the wave packet dynamics by suitable light fields might occur over an extended period of time, *i.e.*, with a light field continuously interacting with the quantum system during the course of temporal wave packet evolution, finally leading to an optimized reaction outcome.

B. Adaptive quantum control

One of the difficulties associated with any calculation of laser control fields is the complexity of quantum system Hamiltonians. It is a great challenge to obtain the associated PESs accurately and determine the dynamical time evolution correctly, especially if there are more than just very few degrees of freedom. In 1992, Judson and Rabitz[51] proposed a seminal scheme by which the optimal laser pulse shape could be iteratively obtained in an experiment without requiring theoretical knowledge of the system Hamiltonian. They suggested the employment of a learning algorithm that processes the experimental signal obtained from the quantum system upon irradiation with differently shaped electric light fields. In the course of optimization, this algorithm would then suggest a number of other pulse shapes subsequently applied to the system, with iterative improvement of the outcome so that at the end, the best electric field for the task at hand would be found without requiring mechanistic input from the user at the beginning. Due to the high flexibility of this approach, a number of ''conventional'' control schemes or combinations of them can be potentially revealed during the process, thus encompassing most of the previously suggested approaches. This concept is often labeled ''adaptive femtosecond quantum control,'' ''closed-loop control'' or ''optimal control experiment''.

The experimental realization of a number of quantum control schemes requires means for generating differently shaped electric light fields in a very flexible manner. This was made possible by the development of so-called pulse shapers.[52,53] With their help, the spectral phase,[54] phase and amplitude,[55,56] and phase and polarization[57] of ultrashort laser pulses can be efficiently modulated (for details, see section IIB). Due to their high flexibility, pulse shapers opened the way to test both ''traditional'' (single-parameter) control schemes as well as implement the adaptive concept.

The first experimental demonstration of adaptive control was carried out in 1997 by Wilson and coworkers.[58] They maximized the fluorescence efficiency and the fluorescence yield of dissolved dye molecules. Independent realizations of the adaptive concept in the same year by Silberberg and coworkers[8] and by our group[9] demonstrated the automated compression of femtosecond laser pulses. In 1998, our group reported the first experiment on adaptive molecular photodissociation control in the gas phase[59] and Meshulach and Silberberg showed phase-shaping control of two-photon atomic absorption.[60] After these initial experiments, a growing number of demonstrations of the adaptive concept was reported, and the general research field of quantum control is now expanding rapidly.

C. Quantum control in different environments

In this review article we will concentrate on femtosecond quantum control in condensed phase systems. Nevertheless, it is appropriate to mention at this point that a large number of gas phase control experiments have been reported since the first demonstrations. Examples of the earlier work are experiments dealing with photodissociation and ionization,[59,61–68] two-photon absorption detected by fluorescence,[60,69] molecular rearrangement,[64] control of quantum wavefunctions,[70] and high-harmonic generation.[71–74] A number of review articles (see *e.g.* ref. 75–82), chapters and special collections of articles

in books (see *e.g.* ref. 83–88), and complete books[89,90] contain extensive treatments of various theoretical and experimental aspects of quantum control.

Here we will mainly consider the specific challenges, opportunities, and applications of femtosecond quantum control that apply to condensed matter environments. The interaction of quantum systems with their environment (such as solute molecules in a solvent) can strongly differ from the isolated situation (such as in a gas phase molecular beam) where these interactions play a minor role. The couplings and additional dynamical processes may strongly complicate the practical application and the interpretation of quantum control schemes. Nonetheless, these complex systems are highly relevant in many areas of physics, chemistry and biology, and it is fascinating to see how quantum control works in these circumstances.

From a practical standpoint, the transfer of quantum control methods and schemes from gas phase to condensed phase systems also requires some technical extensions and developments. For example, a central issue is the requirement for monitoring the exact result of any light-driven quantum dynamics. In order to steer quantum systems in a certain direction, the outcome of such manoeuvres has to be measurable quantities. Since a number of gas phase techniques (*e.g.* mass spectrometry, photoelectron spectroscopy) are not directly applicable, other methods have to be found. The growing number of successful quantum control implementations in recent years demonstrates that this is indeed feasible, with examples ranging from control of photophysical processes in liquids all the way to biomolecular systems.

D. Brief outline of this review

In this review, we will illustrate the main strategies to affect reactions under condensed phase conditions. We will not cover all experiments that have been conducted by the many research groups worldwide, but we would like to give an overview of the main progress and achievements in the field, and specifically discuss some of our illustrative examples. More specifically, in section II we will present the experimental and some of the theoretical background for quantum control in the condensed phase. The discussion of applications is started in section III with control concepts that are based on the variation of one single parameter of the external light field. Several experimental examples will illustrate how condensed-phase dynamics can be influenced very efficiently and what this is useful for. The high generality of employing complex shaped laser pulses is shown in section IV on multiparameter control, and a summary and outlook are provided in section V.

II. Experimental and theoretical background

A. Specific issues of condensed-phase quantum control

Femtosecond optical control of quantum mechanical systems first of all requires suitable light sources. The most common system for time-resolved experiments is the titanium sapphire laser that emits radiation around 800 nm. Commercially available amplified laser systems offer laser pulse durations in the sub-30 fs regime. In an ideal case, these laser pulses leave the laser system bandwidth-limited (*i.e.*, as short as possible for any given spectral bandwidth), and can then be used in the experiment. Remaining phase distortions can be compensated by pulse-shaping setups (section IIB). Further advantages of Ti:sapphire lasers are the achievable short pulse duration, excellent stability and high output power.[91–93]

However, the central wavelength can only be varied by a small amount. In order to adjust the spectrum to the spectral characteristics of the investigated system, either in one-photon or multi-photon excitation schemes, appropriate frequency conversion can be employed. With parametric amplifiers, a broad spectrum can now be covered, ranging from the near-ultraviolet over the whole visible domain into the infrared region. Especially noncollinear optical parametric amplifiers (NOPAs) provide very broadband tunable radiation.[94–96]

The specific challenges and issues faced when employing femtosecond radiation vary strongly from system to system. In recent years a large variety of different condensed phase quantum control experiments has been carried out, among them work on small molecules such as diatomic halogen molecules in rare gas matrices,[97–99] dissolved I_3^-,[100–103] dye molecules in solution,[58,104–112] semiconductors,[21,22,25] molecular crystals[113,114] and even complex biomolecules[115–128] and biological cells,[129] to give an impression of the diversity. Depending on the problem at hand, different techniques can be employed for monitoring and visualizing the quantum time evolution and/or the reaction outcome. Most of these are optical spectroscopic methods, although in principle other techniques such as nuclear magnetic resonance or electrochemical probes may yet turn out to be useful in this context. One always has to ask what the specificity, sensitivity, and required effort are for any given technique.

An example for an optical signal is the detection of the spontaneous emission yield. The molecules are excited by a pump laser beam to a higher PES, from where emission occurs. The resulting emission is then collected by a lens and detected by a photodiode or photomultiplier (Fig. 1a). This signal is rather simple from the experimental point of view, but as a drawback, it contains no directly accessible information on the temporal evolution of the quantum system. Nevertheless, it can be efficiently used for monitoring excitation probabilities for any laser pulse employed in the experiment. Emission spectroscopy is useful in many applications, such as microscopy of tissue and cells.

Another example of a detection method that is insensitive to the ultrafast temporal evolution but useful to discriminate between the effects of different control parameters is the detection of steady-state absorption changes after irradiation with a suitable control field. If permanent changes are induced by the control process, their outcome is thus measurable. An extension of this is the measurement of optical activity. With the help of this property, the change in enantiomer concentrations (chiral molecules) can be recorded. Controlling chirality in various ways, *e.g.* the chirally selective generation of chemical products from an achiral or racemic precursor, is a topic which has drawn much attention theoretically[130–143] and experimentally[144,145] and is a very interesting field for future control experiments.

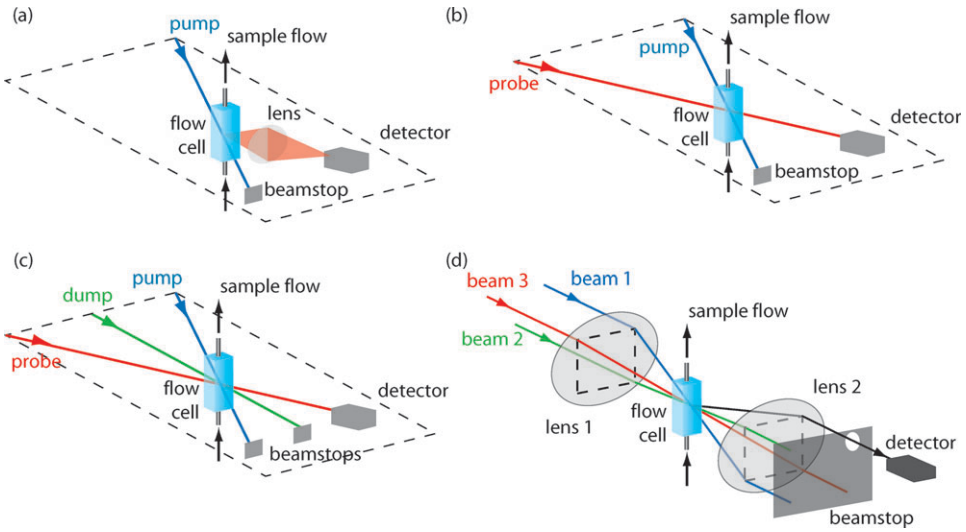

Fig. 1 Different detection schemes used for optimal control experiments, exemplarily for setups employing flow cells. (a) Emission spectroscopy: molecules are excited by the pump beam and the resulting fluorescence is collected and detected. (b) Transient absorption spectroscopy: the system gets excited by a pump pulse and interrogated by a probe pulse which can be delayed with respect to the pump pulse. (c) Pump–dump–probe spectroscopy: the dynamics is initiated by a pump pulse and then influenced by an additional dump (or repump) pulse. The result can again be detected using a probe pulse. (d) Four-wave mixing in boxcar geometry. The direction of the different beams in space needs to fulfil the energy and momentum conservation.

In many cases, where the desired target is either short-lived, or the control objective itself is connected with the quantum time evolution, suitable transient (spectroscopic) methods are required that also monitor the temporal change of physical properties connected with the process. A number of spectroscopic methods fulfil this requirement, each highlighting different aspects connected with the development of the chemical reaction. Depending on the precise control problem, one can employ transient absorption pump–probe spectroscopy, fluorescence up-conversion, Raman spectroscopy, optical Kerr effect measurements, or other four-wave mixing geometries such as photon echo or transient grating, including their heterodyne-detected variants (*i.e.*, coherent two-dimensional spectroscopy).

In transient absorption spectroscopy, the system under study is first excited by a pump pulse and in a second step, the dynamics can be interrogated by a probe pulse that is temporally delayed with respect to the pump pulse (Fig. 1b). Using different wavelengths for the pump and the probe pulse allows one to measure many different aspects of the system. Spectral regions where the absorption of the probe pulse is increased may for example indicate the formation of photoproducts or an absorption from the excited state to even higher states (excited-state absorption), regions of decreased absorption may *e.g.* indicate stimulated emission from an excited state to a lower state.

The induced dynamics can be influenced by one or more additional pulses which are placed temporally between the pump and the probe pulse (Fig. 1c). By this, further excitation (repump process) or stimulated emission (dump process) can be induced. The effect of these additional pulses is then again measured by a probe pulse in a suitable wavelength regime.

Also other schemes that include more than three pulses are very common in time-resolved condensed phase spectroscopy. Fig. 1d shows a so-called boxcar geometry for four-wave mixing (FWM) experiments. Three pulses coming from different directions are overlapped spatially in the sample. The coherent interaction of the three pulses and the sample leads to the formation of a fourth beam conveniently propagating in another direction, which is determined by the phase-matching condition. As will be shown in section IVB many different Raman methods make use of this setup, *e.g.* to measure vibrational dynamics using three degenerated pulses (degenerate four-wave mixing, DFWM).[146] In coherent anti-Stokes Raman scattering (CARS), three pulses of different wavelengths are employed to determine the Raman transitions. Many other spectroscopic FWM approaches exist, too. For transient grating (TG) spectroscopy, two of the incoming beams temporally overlap and write a grating into the medium, at which the third beam is scattered. In photon echo (PE) spectroscopy, the first pulse is scanned temporally with respect to the second. The second and third pulse might arrive at the same time (2-pulse PE), or they also exhibit a variable temporal delay (3-pulse PE). Another application is optical two-dimensional spectroscopy,[147,148] by which vibrational couplings[149–154] or electronic couplings[155] between the energy levels of studied molecular systems can be revealed with infrared or visible pulses, respectively. Depending on the temporal sequence, other information like the polarization dephasing or the population decay times can also be measured with FWM techniques.

A general scheme of condensed phase quantum control can be summarized as in Fig. 2a. An electric control field is applied to the investigated quantum system. This field can be manipulated in dependence on a single or multiple parameters. Dye molecules, oligoatomic molecules or chromophores in proteins can for example serve as quantum systems. The response of the system on the different electric fields has to be monitored

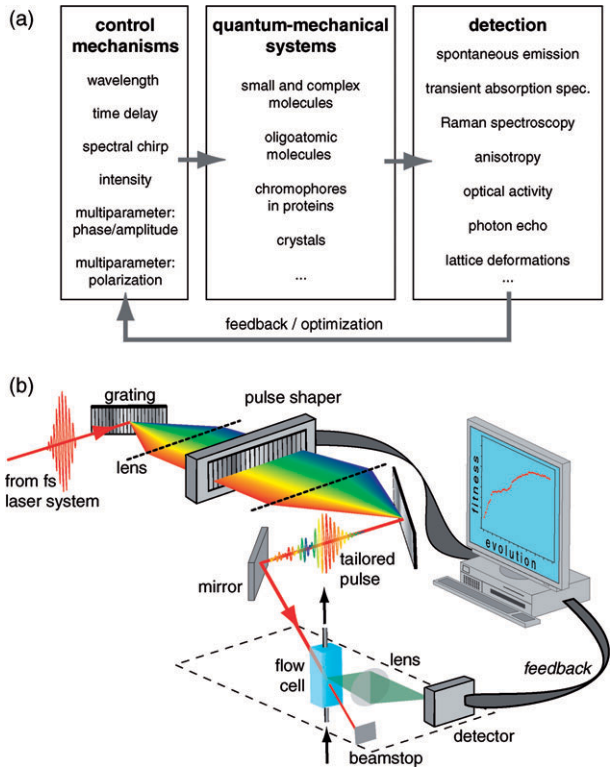

Fig. 2 (a) Scheme summarizing the different control concepts for influencing dynamics in condensed-phase systems. Single- and multiparameter control schemes have been demonstrated on a high number of very different quantum mechanical systems. The result of the different parameter settings can be monitored by various spectroscopic methods according to the given needs. The outcome can be used to find the best parameter values for the given control objective. (b) Illustration of how an adaptive quantum control experiment might look: a femtosecond pulse is shaped in a pulse shaper. The resulting modulated laser pulse is directed towards the experiment. In this example here, the fluorescence of a solvated molecule after excitation with tailored laser pulses is monitored with a detector. The experimental outcome is directly used as feedback by an algorithm which, upon this information, generates new pulse shapes that are applied to the pulse shaper, and eventually finds those especially suited for the given control target.

by suitable methods and the outcome can serve as feedback or it can be interpreted directly. In each control concept, one or more parameters have to be optimized to achieve the best results according to the control objective. In single parameter control methods, the optimal setting can be experimentally determined by scanning the parameter over a reasonable range and measuring the reaction outcome. It is often also possible to theoretically predict the optimal settings that fulfil the control objective.

In the case of multiparameter control concepts, scanning all possible configurations is not feasible. Therefore, learning algorithms are employed to iteratively find parameters that optimize the control objective the best. Fig. 2b illustrates how such a feedback-based algorithm may be combined with an experimental setup. The algorithm generates pulse shapes that are experimentally tested. From these results of a certain number of experiments under different laser pulse parameters, new parameter settings are calculated until further variation of the parameter does not lead to a significant improvement. Therefore, this method is also labeled "closed-loop control" ("adaptive control"). Learning algorithms that are used for this task are for example genetic and/or evolutionary algorithms or simulated annealing.

While this general procedure is the same for gas phase and condensed phase problems, there are also a number of differences. The specific condensed phase techniques for monitoring reaction outcomes have already been mentioned. However, there are also more fundamental challenges associated with condensed phase control schemes because the environment of the quantum systems (*e.g.*, solvents) and their interactions have to be considered. This added complexity may make it more difficult to achieve control objectives under such conditions, but adaptive control is optimally suited to deal with such restrictions in the best possible way.

A prominent example of a control mechanism that is restricted in the condensed phase is the control by high-intensity laser fields. Many experiments have proven that the molecular PESs can be influenced by using intensive laser fields.[68,156–160] Influencing the PESs can then lead to a modified reaction progress and therewith to a different reaction outcome. Although this concept is very successful in the gas phase, the necessary high laser intensities are often not feasible in the condensed phase, because of unwanted nonlinear processes. Beyond a certain intensity threshold, white-light generation will occur in condensed media. Compared to the gas phase, for condensed media the intensity threshold at which white-light generation starts is rather low. The generation of an ultrabroad spectrum which tends to be unstable at high intensities makes it difficult to control processes efficiently under such conditions. Furthermore, the quality of the spectroscopic monitoring signals such as transient absorption or fluorescence spectroscopy will be strongly reduced under conditions in which white-light is generated in the sample. This may occlude the actual process one wants to control, but in certain cases the available control mechanisms may also benefit from such a scenario, as will be seen in section IVB. Finally, too high intensities will lead to heating that can seriously affect and degrade the system (*e.g.* biological molecules). Therefore, quantum control making use of high-intensity effects like Coulomb explosion or strong Stark shifts is in general more restricted in the condensed phase compared to the gas phase.

Another issue concerns the question of decoherence and its relevance under different environments. In the gas phase, it has been demonstrated that photoreactions can be controlled by taking advantage of coherent properties of the laser source and the molecular system. However, it is often argued that while the coherence time is relatively long in the gas phase, it can be significantly shorter in the condensed phase due to the intra- and intermolecular interactions, and thus coherent control concepts would not be useful. In discussing such questions, it is first of all important to clearly define what one means by the word "coherence", as this term tends to be used in different ways in the different scientific communities that contribute to quantum control. Also, one should keep in mind that it is possible and useful to introduce different types

of coherence and their associated timescales. For example, while electronic coherences decay quickly under condensed phase conditions, rovibrational molecular coherences may persist for much longer and can still be exploited in a coherent fashion, as long as they are still present.

A very illustrative experiment, demonstrating vibrational coherence of molecules in liquids, is provided by monitoring the ground state wave packet of I_3^- dissolved in ethanol after excitation with laser pulses at a wavelength of 400 nm. The wave packet motion can be very well visualized by transient absorption spectroscopy at a probe wavelength identical to the excitation wavelength. We have measured the coherent wave packet dynamics as shown in Fig. 3, which is well visible during the first few picoseconds. The reason for this behavior is well understood and both experimentally and theoretically described by Kosloff and coworkers.[100–102] Other very beautiful experiments showing coherent wave packet motion are given, for example, in ref. 161–167. Thus we argue that coherent control schemes are often also applicable in cases where the investigated system interacts with its environment.

B. Femtosecond laser pulse shaping

For optical control the generation of light fields in a very flexible manner is desired such that all the different open-loop or closed-loop schemes can be implemented. In the case of femtosecond laser pulses this means that one should be able to manipulate the phase, amplitude, and possibly also the polarization-state properties with a large number of degrees of freedom. Ultrashort laser pulses can be described in the time domain and in the frequency domain which are connected *via* Fourier transforms, thus shaping of an ultrashort laser pulse can in principle be achieved either in the frequency or time domain.

A very successful technique for femtosecond pulse shaping is based on a so-called 4*f*-setup which allows one to modulate laser pulses in the frequency domain.[52,53] Different implementations of this concept are shown in Fig. 4. The incoming laser beam gets dispersed by a grating. The dispersed beam is then collimated by a lens with a focal length *f*. The grating itself is positioned in the focal plane of this lens. In this way, the individual frequency components will be focused individually, but spatially displaced with respect to each other, into the focal plane of the lens. In this "Fourier plane" the different frequency components can be influenced separately by various methods. A symmetrically arranged second lens and grating recombine the different spectral components. In the ideal case and without further optical components, a laser pulse leaves this geometry without modification. This setup is hence called "zero-dispersion compressor".[168] Instead of gratings, prism-based setups[169–171] are also employed, having the advantage of being applicable for octave-spanning spectra.

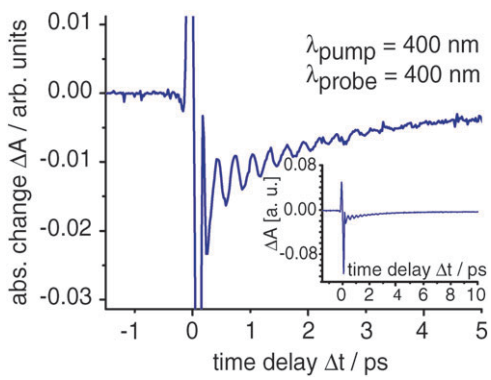

Fig. 3 The molecule I_3^- dissolved in ethanol can be excited at 400 nm to the first excited PES. Depending on the laser pulse parameters this can induce a ground state wave packet which can be monitored at a probe wavelength of 400 nm. The figure shows the transient absorption signal of I_3^- dissolved in ethanol at a probe wavelength of 400 nm. The molecule is excited by a 80 fs laser pulse at 400 nm. The induced coherent ground state wave packet motion can be very well observed by the oscillatory component in the transient.

The actual pulse shaping occurs by suitable spectral modifications in the Fourier plane, employing a spatial light modulator (SLM). Depending on the type of SLM, the zero-dispersion compressor setup may have to be modified slightly with respect to the principal description given above. The most widely used SLM is a liquid crystal display (LCD)[52,172,173] (Fig. 4a). It consists of two glass plates that are coated with small areas of indium–tin oxide, a transparent but conducting substance. These areas represent individual pixels to which electric voltages can be applied. The resulting electric field reorients the long-stretched liquid crystal molecules between the two glass plates and thus modulates the refractive index for transmitted light. The resulting optical path-length difference is thus adjustable for each wavelength in the Fourier plane and enables spectral phase modulation. With the help of two LCD layers and polarizers, one can also achieve independent phase and amplitude control over the wavelength components.

A further development of LCD-based pulse shaping initially shown in our group is ultrafast polarization control.[57,174–187] With this technique it is possible to modulate light fields such that not only amplitude and phase change in an ultrafast manner as a function of time, but also the polarization state (*i.e.*, degree of ellipticity and elliptical orientation) varies within a single femtosecond laser pulse.

Recently, two-dimensional (2D) liquid crystal-based pulse shapers have been introduced[188] and employed in a number of experiments.[28,73,74,189–193] These devices are capable of shaping the femtosecond laser pulse both in time and space, or in two spatial dimensions, allowing direct wavefront shaping. Furthermore, they can also be employed to shape several beams temporally.

Another device employed in 4*f* pulse shaping is the acousto-optical modulator (AOM),[56,194] using diffraction in an appropriate crystal by an acoustic wave which can be externally controlled. The diffracted part of the laser pulse is modulated according to the acoustic wave (Fig. 4b) and thereby allows spectral amplitude and phase shaping.

The spectral phase can also be modulated by geometric elongation or shortening of the optical path between the different frequency components. This can be achieved by deformable mirrors, whose membrane surface can be deformed either electrostatically by small electrodes[13,17,195,196] or by small piezo-motors[197] (Fig. 4c). These setups always lead to a smooth phase function, while other realizations with

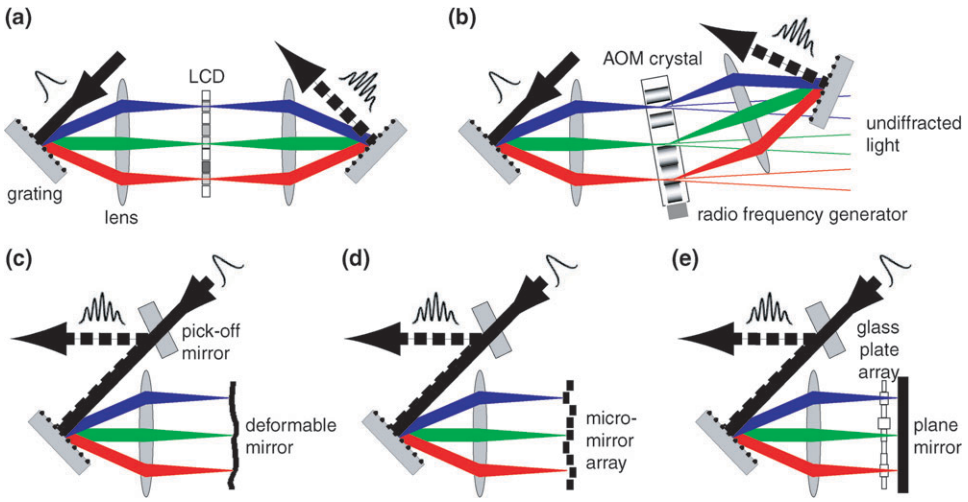

Fig. 4 Different pulse-shaper realizations based on 4*f*-setups (zero-dispersion compressors); (a) liquid crystal display SLM, (b) acousto-optical modulator SLM, (c) deformable mirror, (d) micromachined deformable mirror, (e) glass-plate SLM. The incoming laser pulse (black solid line) is dispersed by a grating, while a lens produces parallel, differently colored beams. Each of them is individually focused into the Fourier plane, where the actual pulse shaping occurs with one of these SLMs. After travelling an analogous path to the one towards the Fourier plane, the laser pulse (black dashed line) leaving the 4*f*-setup is modulated in the desired way.

micromirror arrays consisting of small individual mirrors[198,199] (Fig. 4d) are pixelated and thus can be used to impose spectral phase steps.

In a more exotic realization, the ultrafast laser pulse is shaped by modulating the optical path with the help of small glass plates, which are located directly in front of the Fourier plane.[200,201] By rotation of the glass plates, the optical path length is changed and thus, the spectral phase can be modulated (Fig. 4e).

With the help of an acousto-optical programmable dispersive filter (called "Dazzler"),[202] the laser beam can also be shaped in the time domain, without using a 4*f* geometry. Like the acousto-optical modulator, the Dazzler utilizes the birefringence of AO crystals, but along the propagation direction of the light. As it is a time-domain technique, the laser and the acoustic wave have to be synchronized most accurately, which is very difficult, especially for very short pulses. However, the Dazzler is a very useful and simple to use device for smooth phase functions, while more complex laser pulse shapes are more challenging with a Dazzler.

For polarization shaping on a femtosecond timescale, LCD pulse shapers are unrivalled so far. In other cases, depending on the control problem, but also depending on the wavelength regime, different types of pulse shapers are more or less appropriate. For example, many molecules have absorption bands in the ultraviolet (UV) region that one might wish to exploit, or then again vibrational transitions that would have to be addressed in the mid-infrared (MIR). Therefore it is often desirable to shape laser pulses at these wavelengths. Commercially available liquid crystal SLMs for example are not transmissive in UV or MIR wavelength regions and hence cannot be used to shape laser pulses at these wavelengths. Nevertheless, indirect shaping techniques have been developed; laser pulses can be modulated in spectral regions accessible with standard SLM techniques and their properties can then be transferred to other wavelengths by frequency conversion. Recent progress has also been made in direct UV shaping with micromirror arrays and acousto-optical techniques,[199,203,204] and direct IR shaping with AOM-based devices.[205–212] One can conclude that either by direct or indirect laser pulse shaping, modulated laser pulses are now available spanning a spectral region from a few nanometers up to tens of micrometers, from the deep UV (including shaping of high harmonics, which has been recently demonstrated[71–74,191]) over the UV,[61,109,199,203,204,213–217] visible and near-infrared to the MIR.[205–212] The technology for achieving quantum control with shaped laser pulses under many different conditions is thus developed and can be employed appropriately.

III. Single-parameter control

Several very efficient single-parameter quantum control schemes have been developed and experimentally verified in the condensed phase. In this section we will discuss some of these concepts and their applications to both small and large systems. The examples are also valuable for understanding the multiparameter control schemes presented in section IV.

A. Wavelength control

As already stated in the Introduction, wavelength control using highly monochromatic and tunable laser sources has very early been thought to have potential for selective bond breaking. Unfortunately, due to the rapid intramolecular vibrational redistribution of the deposited energy these concepts were not as successful as initially hoped.

Despite these difficulties, choosing the correct irradiation frequency can still have a very decisive impact on the outcome of a photochemical reaction. The simplest effect due to scanning the wavelength is a greater number of excited molecules and therewith, in general, a higher product yield if the

excitation frequency matches the maximum of the absorption spectrum. Besides this more or less trivial effect, excitation with different wavelengths will induce wave packets at different spots on the addressed PES. As a consequence, the reaction progress and hence the product outcome can be different. Moreover, a higher excitation energy also allows the population of energetically higher-lying states which can have a decisive impact on the following dynamics and therefore result in a different reaction outcome.

A change in reaction progress with excitation wavelength has been reported for different systems. In 1986, the group of Sundström demonstrated that changing the wavelength of the pump pulse results in an excitation to different regions on the first excited surface.[218] The creation of a wave packet at different positions of the first excited state can then significantly influence the forthcoming dynamics. This issue was investigated for the isomerization process of the molecule 1144C dissolved in hexanol and decanol.

Vöhringer and coworkers reported a dependence of the different dissociation product channels of the relatively small molecular system I_3^- on the excitation wavelength.[219] If this system is excited by 400 nm photons, dissociation into I and I_2^- occurs. In contrast, when excited at a wavelength of 266 nm, three-body dissociation can be monitored additionally, hence leading to $I + I + I^-$. The high- and low-energy excitation will result in a transition to different electronic states. 400 nm light exclusively excites a lower excited state while light with a wavelength of 266 nm preferentially excites an upper excited state. From the state which is populated by 266 nm light, an effective pathway to three-body dissociation is available. This pathway leads, over a transition state of the bimolecular reaction (diiodide/iodine), to the final three-body dissociation product.

Varying the excitation wavelength may also have an effect for highly complex systems, leading to different reaction paths. The group of van Grondelle used this control concept on the photoactive yellow protein, which is responsible for initiating the ''blue-light vision'' of *Halorhodospira halobia*.[120] Excitation with 395 nm light initiates an ionization pathway that coexists with the common photoactive yellow protein photocycle. This ionization pathway leads to the production of a radical and an electron, ejected into the protein pocket. The accessibility of the ionization pathway strongly depends on the wavelength that is used for the pump pulse. While the corresponding signature of the ionization is present in the transient absorption signal for a pump pulse wavelength of 395 nm, it cannot be seen if the system is excited by 470 nm light, inducing only the common photocycle. The group's experiments indicate that a resonance-enhanced two-photon transition is responsible for this behavior. In both cases of excitation with 470 nm and 395 nm laser pulses, the first excited surface is populated. Due to the different photon energies of 470 nm and 395 nm light, the initial Franck–Condon regions, where the wave packet is created first, will differ. A second photon can now excite the molecule from the first excited PES to an even higher-lying state. For the case using a pump pulse at 395 nm, the ionization potential of the chromophore can be exceeded, which is not possible for light at a wavelength of 470 nm.

A very nice application for wavelength control is the improvement of contrast ratio in fluorescence microscopy of living organisms, as *e.g.* demonstrated by the group of Joffre with a Dazzler pulse shaper.[129] In that experiment the pulse shaper was only used to modulate the excitation spectrum to produce pulses which are blue-shifted or red-shifted with respect to each other. Chromophores with different excitation spectra can thus be selectively excited. With a Dazzler (as well as with an AOM pulse shaper based on a 4*f*-setup, see Fig. 4b) it is possible to switch between the different laser pulse shapes much faster than with current liquid crystal-based pulse shapers. This makes it possible to acquire two images quasi-simultaneously which correspond to different fluorescent chromophores in the sample. Because of this quasi-simultaneous acquisition, there is a perfect pixel-to-pixel spatial correspondence between the two images. Therefore, linear combinations of the two pictures can be analyzed, which improve the contrast ratio significantly. This concept has been applied to two-photon excited fluorescence images of a *Drosophila* embryo labeled with an enhanced green fluorescent protein. Fig. 5a shows the two-photon excited fluorescence image for the case of excitation with bandwidth-limited laser pulses. The two-photon excited fluorescence image, using the previously described method of linear combination of two quasi-simultaneously acquired images with spectrally shaped laser pulses, is displayed in Fig. 5b. By comparing the two images, it can be seen that the spectral shaping method provides a much better contrast ratio.

In section IV, we will see that it is also possible to enhance the fluorescence efficiency of certain individual chromophores with adaptively shaped laser pulses. A higher fluorescence efficiency means that the absolute fluorescence yield is higher for a certain pulse shape compared to the absolute yield of unshaped laser pulses of the same energy. It has also been demonstrated that in the case of two-photon excitation, it is possible to change the ratio of fluorescence yields from different types of chromophores even if the linear and two-photon absorption spectra are identical.[105] Such laser pulse shapes can be used to further improve the contrast ratio in

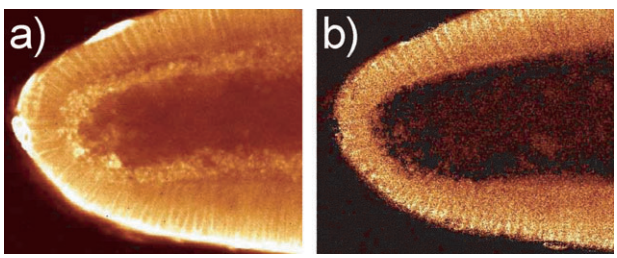

Fig. 5 Two-photon excited fluorescence images of a *Drosophila* embryo labeled with an enhanced green fluorescent protein. (a) Excitation with bandwidth-limited laser pulses, (b) linear combination of two quasi-simultaneously acquired images with different excitation laser pulse shapes. These laser pulses mainly differ in their central wavelength, so that as a consequence different chromophores are preferentially excited. As can be seen, the spectral shaping method leads to a much better contrast ratio. Adapted from ref. 129 with permission from the authors and from the Optical Society of America. Copyright 2006 Optical Society of America.

fluorescence microscopy and help recording detailed pictures of living organisms.

B. Control by spectral interferometry

With multipulse excitation, it is possible to achieve wavelength-type control if two laser pulses that overlap spectrally are used for the excitation step. This will affect the overall spectrum by causing spectral interferences and thus has an influence on the wavelength-sensitive processes. An example can be seen in Fig. 6, showing two pulses with identical individual spectra, but with a temporal separation. The combined spectrum (as it will *e.g.* be measured by a spectrometer) exhibits spectral interference. This means that there are spectral regions where the probability of finding a photon is zero, although for either pulse in the absence of the other one, the probability is not zero, a clear indication for destructive interference in the spectral domain. Analogously, for certain wavelengths the intensity is four times as high as for one pulse alone, due to constructive interference. The interference pattern depends on the time separation and the relative phase of the two employed pulses (and of course on their spectra).

This spectral interference effect has to be taken into account if experiments are performed in which two excitation laser pulses of overlapping spectra are employed. For instance, the absorption of an atomic transition can be easily increased if the two pulses are adjusted so that there is constructive interference at the transition wavelength.

If just one pulse is employed and only the spectral phase of the laser pulse is modulated, a spectrometer will always measure identical spectra, because it works in the linear regime. However, one has to keep in mind that the spectral phase does not influence the spectral amplitude, but both the temporal amplitude and phase. In contrast, for experiments in the nonlinear regime, *i.e.* with multi-photon interactions, the spectral phase can strongly influence the outcome of the experiment. For instance, in a two-photon process, the decisive spectral distribution is the second-order power spectrum

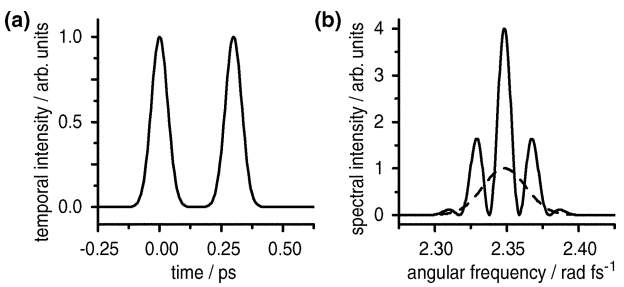

Fig. 6 Scheme illustrating the effect of spectral interference: (a) a bandwidth-limited Gaussian-shaped femtosecond laser pulse (central wavelength λ_0 = 800 nm, spectral width $\Delta\lambda$ = 12 nm), and an identical copy 300 fs after the first pulse. (b) The combined spectrum of these two pulses. The spectrum of each individual pulse in the absence of the other is indicated by a dashed line. If both impinge on a spectrometer, the interferences can be observed. In an experiment, techniques based on this effect can be used to enhance transitions *via* constructive, or suppress them *via* destructive interference, respectively. The scenario outlined in this figure can be understood as a time/energy domain analogue to Young's double slit experiment, which takes place in the position/momentum domain.

(SOPS), directly related to the Fourier transform of the square of the temporal electric field, and thus strongly dependent on the spectral phase of the laser pulse.[220] This opens the door to a manifold of control scenarios with phase-shaped laser pulses.

Some illustrative examples are presented in Fig. 7 for a pulse with a Gaussian spectrum centered at ω_0. The spectrum and the spectral phase are shown in the first column, while the respective temporal intensity profile can be seen in the second column. Due to the spectral width of the pulse, both sum-frequency generation (SFG) and difference-frequency generation (DFG) of two frequencies comprised by the spectrum can be generated in a nonlinear process of second order. This leads to contributions in the region around $2\omega_0$ (fourth column of Fig. 7) and at the region close to the origin of the frequency axis (third column of Fig. 7). The former are important *e.g.* in two-photon transitions or SHG, the latter can be employed for stimulated Raman scattering experiments or the generation of MIR pulses. The rows in Fig. 4 represent different spectral phase patterns as discussed in the following.

An unmodulated spectral phase results in a bandwidth-limited Gaussian profile in the time domain (Fig. 7a2). The corresponding contributions in the SOPS (Fig. 7a3) are Gaussian shaped, too. A sinusoidal spectral phase pattern (Fig. 7b) leads to a temporal pulse train. In its SOPS, both in the SFG and the DFG process, certain frequencies can be selectively suppressed. The distance of the peaks in the SOPS reflects the temporal spacing of the subpulses in the pulse train, and is thus directly controllable *via* the spectral phase pattern. A triangular spectral phase (Fig. 7c) creates a double pulse whose subpulses are composed of different spectral contributions. In the SOPS, the modulations in the DFG region (also called the "optical rectification" region) around $\omega = 0$ reveal the temporal separation of the two subpulses, while around $2\omega_0$, one can basically see the sum of the SHG spectra of the two subpulses. Shaping the spectral phase can be used to easily narrow the SOPS to a certain frequency (or to exclude certain frequencies from the SOPS), thus facilitating wavelength-selective two-photon excitation. Very simple spectral phase patterns (like the third-order polynomial shown in Fig. 7d) can already be employed to achieve this effect. All the examples shown in Fig. 7 have been applied experimentally to control second-order processes, and many of them will be discussed in the following sections.

In an impressive work, Meshulach and Silberberg investigated the effect of tailored pulses on the two-photon absorption of Cs gas.[60,69] The two-photon transition at a wavelength of 411 nm was induced by phase-shaped femtosecond laser pulses centered at 822 nm. They concluded that certain pulse shapes do not excite the atomic system at all, while others can cause the same emission yield as bandwidth-limited pulses. Intuitively one might have expected that the shortest pulse with the highest pulse intensity also results in the highest two-photon excitation probability. In contrast, experiments and theory show that pulses with a double hump, induced by a π phase step at the central wavelength of the pump pulse, can also excite the system with the same efficiency as bandwidth-limited pulses. They also showed that this mechanism works in the narrow-line limit, where the absorption line is much narrower than the excitation spectrum, but not in cases with

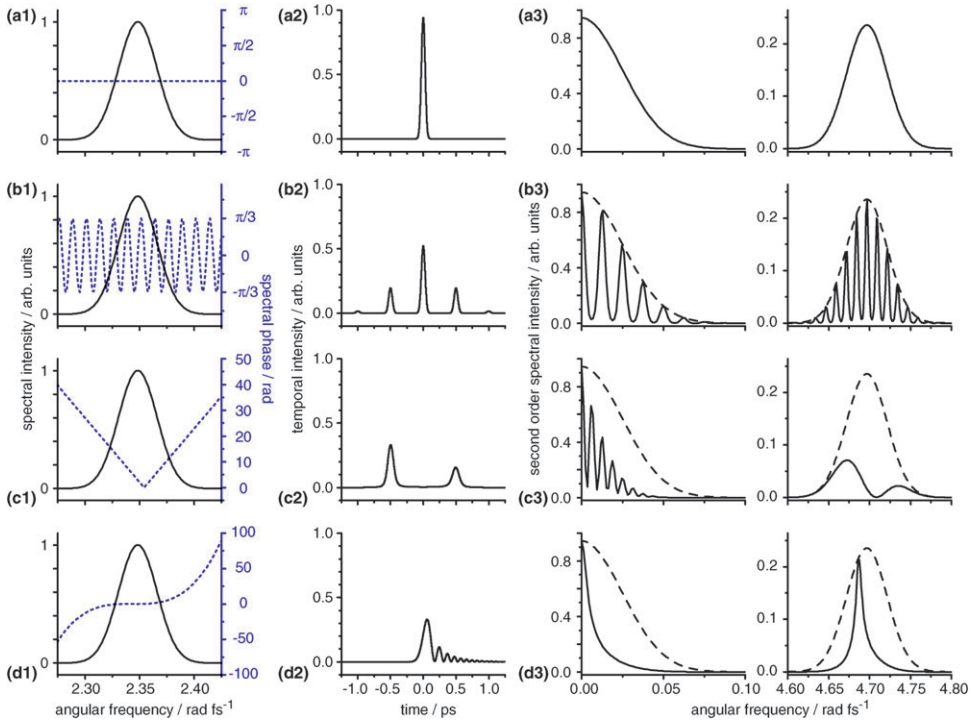

Fig. 7 Examples for phase-modulated laser pulses with Gaussian spectrum centered around $\lambda_0 = 800$ nm and having a spectral width of $\Delta\lambda = 12$ nm. The electric field is described as $E(\omega) = A(\omega)\exp[-i\phi(\omega)]$, where $A(\omega)$ is the spectral amplitude. Spectral intensity $I(\omega) \propto |E(\omega)|^2$ (first column, black solid line) and spectral phase $\phi(\omega)$ (first column, blue dotted line), temporal intensity profile (second column) and the intensity (amplitude square) of the SOPS (third column for DFG, fourth column for SFG) are shown for four different spectral phases. The SOPS of the unmodulated laser pulse is also shown as a dotted line for comparison. The four spectral phases are: (a) $\phi(\omega) = 0$: unmodulated spectral phase, creating a bandwidth-limited laser pulse; (b) $\phi(\omega) = \pi/3\sin[500\text{ fs/rad}(\omega - \omega_0)]$: a sinusoidal phase, creating a pulse train; (c) $\phi(\omega) = -500\text{ fs}(\omega - \omega_0)$ for $\omega < 2.36$ rad fs^{-1} ($\lambda > 798$ nm), $\phi(\omega) = +500\text{ fs}(\omega - \omega_0)$ for $\omega > 2.36$ rad fs^{-1} ($\lambda < 798$ nm): a triangular spectral phase, creating a colored double pulse whose first subpulse is higher in intensity and consists of lower frequency components than the second one; (d) $\phi(\omega) = 1/2(5000\text{ fs}^2)(\omega - \omega_0)^2 + 1/6(10^6\text{ fs}^3)(\omega - \omega_0)^3$: a polynomial spectral phase of third order, creating a pulse train with decreasing subpulse intensity.

very broad inhomogeneous line shapes. The latter investigations were performed on coumarin 6H in ethanol (60 nm absorption width) with laser pulses of 14 nm spectral width. Scanning the π-phase step for this dye molecule showed that this time, the bandwidth-limited pulse with the highest intensity also has the highest two-photon transition efficiency,[69] *i.e.*, the highest intensity causes the largest two-photon excitation yield.

These experiments can be nicely explained with the help of the dependence of the SOPS on the spectral phase of the first-order spectrum (Fig. 7). For certain parameterizations of the spectral phase, the second-order power spectrum has no amplitude at the frequency necessary for the transition, thus preventing the system from getting excited at all. This can only happen if the absorption profile of the system is narrow enough to lie completely in a minimum of the SOPS. Such a condition can be easily satisfied for atoms, but not for complex molecules which have very broad inhomogeneous line shapes.

Similarly for a *n*-photon transition, the *n*-th order power spectrum has to be considered in order to interpret the results. As already mentioned, DFG processes are relevant for multi-photon transitions that include stimulated emission/dump processes. This is, for example, the case for Raman-type experiments, where ground state vibrational modes can be selectively populated. The population of ground state vibrational modes can occur *via* the absorption of a photon from the blue wing of the spectrum and a consecutive stimulation by a photon of the red wing of the spectrum. Certain spectral phases can eliminate any amplitude in the respective region of the SOPS (Fig. 7, third column). If a vibration corresponds to such a frequency, it will not be excited. By this mechanism, selective excitation of different vibrational modes can be easily understood.

The spectral phase of the employed pulses also has the potential to influence the system under study beyond power spectrum control. The formation and evolution of the induced dynamics after the interaction with the laser may be sensitive to phase information, opening the possibility of actively controlling molecular dynamics *via* pulses adaptively shaped in phase and amplitude. The following sections will contain several experiments revealing the necessity of the phase of the electric field for the control mechanism.

C. Pump–dump control

After successful implementation in gas phase experiments,[35–37] pump–dump control has been applied to several different problems in the condensed phase, too.[102,103,115–117,120–124,128,221–225] The concept is generally divided into three steps: excitation of the system with the pump

pulse, a second interaction after a certain period of time with the dump pulse, and the final detection step (Fig. 8). In some gas phase experiments the second pulse acts both as the controlling dump pulse as well as the detection pulse. The time delay between the first and the second laser pulse represents the control parameter, which governs the reaction outcome. Although this concept is generally labeled a pump–dump scheme, instead of dumping the population to a lower state, the population can also be transferred to higher excited states or be re-pumped after having repopulated the ground state PES.

Different reaction channels can be accessed selectively depending on the pump–dump delay time. The time delay often provides valuable information about the reaction process. An early application of pump–dump and pump–repump control, respectively, in liquids has been demonstrated by Troe and coworkers in 1995 on stilbene in *n*-pentane and methanol.[221] This very well investigated molecule can undergo *cis–trans* isomerization or, as an alternate channel, perform an electronic rearrangement process and form dihydrophenanthrene (DHP).[226] In the experiment of the Troe group, *cis* stilbene is excited onto the first excited (S_1) PES, where it can isomerize to form *trans* stilbene. This process occurs rapidly within 0.5 ps when methanol is used as solvent and within 1 ps in the case of *n*-pentane. With a second laser pulse the *trans* stilbene molecules produced are re-excited to the S_1 PES. The resulting fluorescence is collected and monitored in dependence on the time delay between the first and second laser pulse. This probe signal is proportional to the amount of excited *trans* molecules. The highest fluorescence yield is obtained for a delay time of 10 ps for stilbene in methanol and about 15 ps for stilbene dissolved in *n*-pentane. The temporal evolution of the fluorescence signal thus reveals the cooling process of the *trans* stilbene molecules produced. This experiment nicely illustrates a specific example that pump–dump and pump–repump schemes can be utilized to influence molecular dynamics by selective re-excitation of a certain reaction channel.

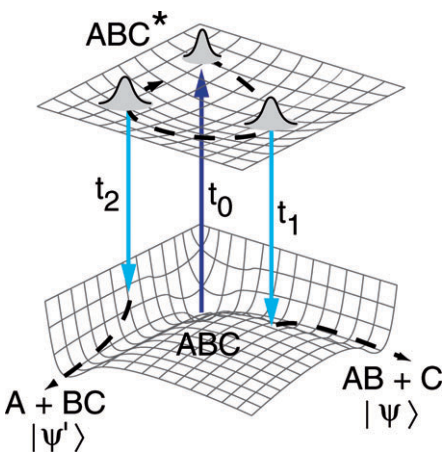

Fig. 8 Sketch of the Tannor–Kosloff–Rice scheme.[32,33,35,76] A wave packet is created on the first excited PES by an ultrashort pump pulse. With the help of a second laser pulse of the proper wavelength and time delay with respect to the excitation event, the wave packet can be dumped into the desired product channel.

Due to the relatively long time duration between the pump and the dump pulse of up to several tens of picoseconds in the previously discussed example, coherent wave packet motion does not play a key role in that specific case. This is different in two other experiments reported by the group of Anfinrud[115] and by Ruhman *et al.*,[117] which take advantage of the position of the wave packet on the S_1 PES. They investigated the molecule retinal embedded in the protein bacteriorhodopsin. Following photoexcitation, this molecule undergoes an isomerization reaction from the all-*trans* to the 13-*cis* configuration. The amount of produced 13-*cis* isomers and the stimulated emission signal of the excited molecules are investigated with regard to the dependence on the temporal position of a second pulse (the dump pulse) which induces a transition from the S_1 PES back to the ground state (S_0) PES (and a contribution of excited state absorption as well) close to a conical intersection. To probe the dump-pulse effect on the 13-*cis* isomer yield, transient absorption spectroscopy is employed. Without the dump pulse, the initially excited wave packet will evolve on the S_1 PES (where fluorescence can occur) and reach a conical intersection, where it can descend to the S_0 PES. This transition through the conical intersection leads with 35% probability to the *trans* isomer, while in 65% of all excitations with unshaped light, the 13-*cis* isomer is formed.[166] With a dump pulse, part of the wave packet is transferred back to the S_0 PES (and partially to higher-lying states), before it reaches the conical intersection. This reduces the stimulated emission monitored for times after the dumping act, because the population is transferred back to the ground state, prohibiting any more fluorescence. This can be seen in Fig. 9, showing results from an experiment in which the stimulated emission is measured with and without a dump

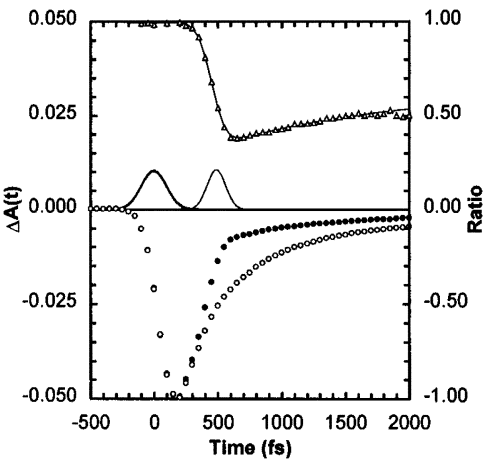

Fig. 9 Pump–dump–probe experiment on retinal in bacteriorhodopsin.[115] Temporal behaviour of the stimulated emission at 900 nm without (open circles) and with (closed circles) a 780 nm dump pulse coming 450 fs after the 600 nm pump pulse. The triangles mark the ratio of the two signals. Also displayed are the instrument response function of the pump and the dump pulses used in the experiment. Reprinted from F. Gai, J. Cooper McDonald and P. A. Anfinrud, *J. Am. Chem. Soc.*, 1997, **119**, p. 6201, with permission from the authors and the American Chemical Society. Copyright 1997 American Chemical Society.

pulse. As a consequence, the amount of 13-*cis* isomers produced will also be reduced, as has been detected in the study by Ruhman *et al.*[117] Besides this control aspect, careful analysis of the corresponding transients provides new information about the early dynamics in the isomerization cycle of retinal in bacteriorhodopsin. This successful control scheme of the retinal photoisomerization reaction in bacteriorhodopsin has been extended recently by additional pulse shaping of the dump pulse,[128] as will be discussed in section IVC.

Extensive pump–dump studies have been performed on the photoactive yellow protein system and derivates by the group of van Grondelle.[120–124] Similar to the experiments discussed above, van Grondelle and coworkers investigated the change in stimulated emission and the bleach recovery dependence on the time delay between a pump and a dump pulse connecting the S_1 and S_0 PESs. The stimulated emission drops in the presence of a suitable dump field and consequently, the bleach signal is reduced as well due to the repopulation of the ground state. While in general both signals are strictly correlated, this is not the case for the given molecular system and thus part of the dumped population is not directly transferred to the ground state by the dump pulse, but to another ground-state intermediate state. Such a ground-state intermediate state cannot be detected by pure transient spectroscopy methods. This example demonstrates the potential of identifying and manipulating molecular dynamics with the help of pump–dump schemes for the yellow protein and derivate systems even without exploiting the dependence of a product signal on the delay time to achieve quantum control.

Laser pulse sequences can also be used to generate certain desired transient chemical species for further investigation if they are not available otherwise. This is for example necessary if the dynamics of the molecule I_2^- dissolved in ethanol are the point of interest,[103] which can be produced by irradiation of I_3^- with light of the proper wavelength. After thermal equilibration the produced I_2^- is available for spectroscopic studies. Further laser excitation finally results in dissociation of I_2^- into I^- and I.

Due to its potential for controlling chemical reactions and providing insight into reaction mechanisms, the pump–dump scheme is a widely applied concept. The induced dynamics can easily be explained in the time domain and often an intuitive interpretation of the control mechanism is possible. The efficiency of chemical reactions often depend sensitively on multipulse control schemes. To obtain an optimized reaction yield, other parameters such as the wavelength or the shape of the individual laser pulses have to be optimized, besides the temporal spacing of the laser pulses. This can be done efficiently by multiparameter control schemes (section IV).

D. Control with linear chirp

In various experiments chirped laser pulses have proven to be essential to optimize the dynamics of different condensed phase systems.[58,97,104,164,227–236] A simple way to produce a linearly chirped laser pulse is to generate a second-order spectral phase with an adequate pulse shaper. Earlier experiments often employed a setup of two gratings or two prisms in a folded geometry that could be adjusted in order to introduce chirp. Also, simply sending the laser pulse through dispersive material leads to a positive linear chirp.

Chirped laser pulse excitation has a strong impact on the excited-state population of solvated molecules. This effect was first investigated by Shank and coworkers.[228] In a high-intensity regime, the number of excited molecules can be enhanced using positively chirped laser pulses, and reduced with negatively chirped laser pulses. This observation can be interpreted within the Tannor–Kosloff–Rice pump–dump scheme presented in section IIIC. Molecules for which the S_0 and S_1 minima do not coincide with respect to the reaction coordinate can have a non-equilibrium population in the S_1 state after excitation that moves from higher to lower potential energy gaps between S_1 and S_0. This causes a shrinking energy separation of the PESs with respect to the center of mass of the wave packet. In a negatively chirped laser pulse, the light frequencies decrease with time. Therefore, the temporal frequency arrangement follows the energy separation marked by the wave packet's center of mass. A second interaction with the excitation laser pulse can thus dump a certain fraction of the amplitude back to the ground state. This effect is suppressed in the case of positive chirp values in which the low frequencies come first and the high frequencies come last (Fig. 10a).

An example for this behavior is presented in Fig. 10b for the dye molecule IR140 (5,5′-dichloro-11-diphenylamino-3,3′-diethyl-10,12-ethylene thiatricarbocyanine perchlorate) dissolved in methanol, excited with differently chirped 800 nm laser pulses as performed in our group.[237] To get a signal

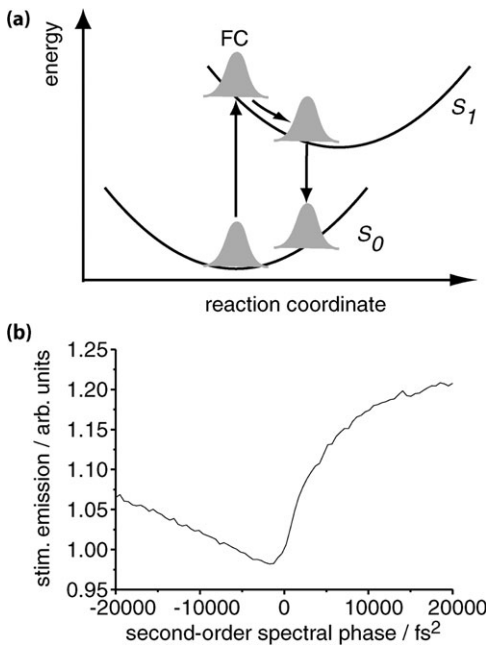

Fig. 10 Intrapulse pump–dump chirp control. (a) Scheme of the potential energy surfaces illustrating the intrapulse dumping and pump–dump mechanisms. The excited state wave packet is initially created in the Franck–Condon (FC) region of the S_1 PES. Due to intrapulse dumping, the fluorescence yield is higher for positively chirped laser pulses than for negatively chirped laser pulses. (b) Dependence of the stimulated emission of the molecule IR140 on the second-order spectral phase in a high-intensity regime.[237]

proportional to the amount of excited-state population, the stimulated emission at 870 nm is measured in a transient absorption experiment. The presented curve agrees well with the theoretical and experimental findings of other groups concerning comparable systems.[58,228,230]

Similar experiments have been performed on other dye molecules[228] and also on biomolecular systems.[230] The findings of these experiments are especially interesting with respect to the interpretation of multiparameter experiments, in which the laser-induced fluorescence yield is chosen as control objective.[58,112] This observable is proportional to the excited-state population and therefore the above mechanism must be considered in the interpretation of the optimal laser pulse shapes.

In a further experiment the group of Shank investigated the selective excitation of wave packet motion using chirped laser pulses.[227] Very often emission and absorption bands of molecules strongly overlap. Pump–probe signals in this regime will reflect both the excited state as well as the ground state dynamics. A very short exciting laser pulse induces a wave packet on both S_0 and S_1. In analogy to the above discussed intrapulse dumping mechanism, chirped laser pulses can enhance or reduce the different oscillating components. Down-chirped laser pulses, which have proven to efficiently dump the excited-state population, will favor the creation of a non-stationary ground-state hole,[164] because several vibrational levels on S_0 can be populated with S_1 as an intermediate state (an impulsive resonant Raman process, see also section IVB). Therefore, a ground state oscillatory component to the overall signal will be increased when down-chirped pulses are used for the excitation. The effect is the opposite for positively chirped laser pulses, where the temporally increasing laser frequency leads to excitation of higher-lying S_1 states rather than a dump mechanism back to S_0.

As the vibrational dephasing time depends on the region of the PES and the given electronic state, this different behavior for oppositely chirped pulses can be visualized. For the molecule LD690 (which exhibits a 586 cm^{-1} ring-breathing mode) dissolved in methanol the dephasing time for low-lying vibrational states of S_1 is roughly 3 ps, for low-lying vibrational states of S_0 at least 10 ps, and for higher vibrational states about 1 ps for both the S_0 and the S_1 PES.[227] Down-chirped pump pulses can cause oscillations (dominated by S_0 contributions) in the measured signal that are significantly different from those for up-chirped pulses (where S_1 contributions dominate). This is illustrated in Fig. 11, where the probe wavelength is set to the blue edge of the pump pulse spectrum. For up-chirped pump pulses, the measured signal reflects the decay of high-lying vibrational S_1 states, while for down-chirped pulses, the oscillations originate from lower-lying S_0 states and therefore persist for a longer time. Several groups performed this kind of experiment on various dye molecules[227,232,236] and even on the complex system retinal within bacteriorhodopsin.[164]

With chirped laser pulses, selective excitation of wave packet motion and control of the amount of excited molecules and the shape of the induced wave packet are possible. Bardeen *et al*. showed that the spreading of propagating wave packets can be counteracted by the chirp of the pump laser

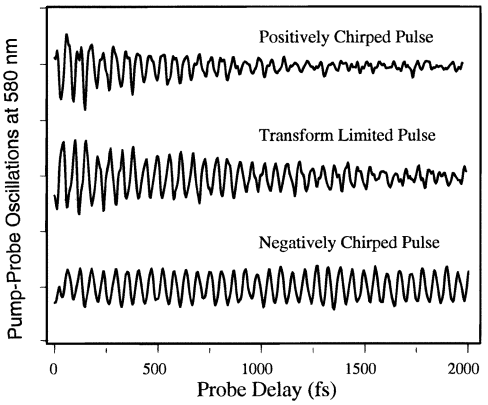

Fig. 11 Experiment on the selective excitation of wave packets.[164] Transient absorption signal of the molecule LD690 dissolved in methanol at a probe wavelength of 580 nm and a pump pulse whose spectrum spans a wavelength region from ≈560–680 nm. The three transients show only the oscillatory component in the case of positively chirped, negatively chirped and transform-limited excitation. Reprinted from C. J. Bardeen, Q. Wang and C. V. Shank, *J. Phys. Chem. A*, 1998, **102**, p. 2759, with permission from the authors and the American Chemical Society. Copyright 1998 American Chemical Society.

pulses.[97] They have investigated the wave packet dynamics of I_2 in a Kr matrix at 15 K, which they have excited with a pump pulse at 565 nm and then repumped at 394 nm. They monitored the subsequent laser-induced fluorescence at 430 nm as a function of the chirp of the pump pulse and of the delay between pump and repump laser pulses. The resulting signal for positively chirped laser pulses shows less structure when pump and repump are a few picoseconds apart than for negative chirp excitation. The PES, on which they induced the wave packet, is anharmonic. The more anharmonic, higher-lying vibrational levels have a longer oscillation period than the components of lower vibrational energy. To have a focused wave packet the higher components must be excited earlier in time than the lower components, which can be achieved with a negatively chirped laser pulse, in which the high frequencies precede the low ones. A positively chirped laser pulse will have the opposite effect. This experiment[97] is a nice demonstration that it is possible to control the shape of the wave packet by shaped excitation laser pulses such that the wave packet is focused later in time at a different position on the PES.

Chirped laser pulses have also proven to be very helpful in coherent anti-Stokes Raman scattering (CARS) experiments. Using laser pulses with a non-zero second-order spectral phase can help improve the resolution in CARS experiments.[234,235] Besides this resolution improvement, chirped laser pulses in CARS experiments can also enable selective excitation of vibrational modes.[233] In these experiments by the group of Kiefer and Materny,[233] performed on diacetylene single crystals, they achieved nearly exclusive excitation of one single mode, while the CARS transient in the case of transform-limited excitation laser pulses showed several features. Employing chirped laser pulses and multiparameter schemes in Raman spectroscopy will be further discussed in section IVB.

An interesting application of chirp control has also been demonstrated on the issue of selective excitation of vibrational levels with the help of a ladder-climbing mechanism. Ladder climbing in the condensed phase has been demonstrated by the group of Heilweil on the molecule $W(CO)_6$ in *n*-hexane solution.[229,238] Using laser pulses in the infrared region, higher-lying vibrational levels can be populated by climbing of a vibrational overtone ladder with several adequate infrared photons. This mechanism has been demonstrated to be dependent on the second-order spectral phase of the pump laser pulse.[229] Unchirped and positively chirped pump pulses lead to predominant population of the $\nu = 1$ level, while with negatively chirped laser pulses significant excess population in the $\nu = 2$ level is produced (Fig. 12). Controlling the population of different vibrational levels is especially interesting with respect to controlling dynamics on the ground state PES.

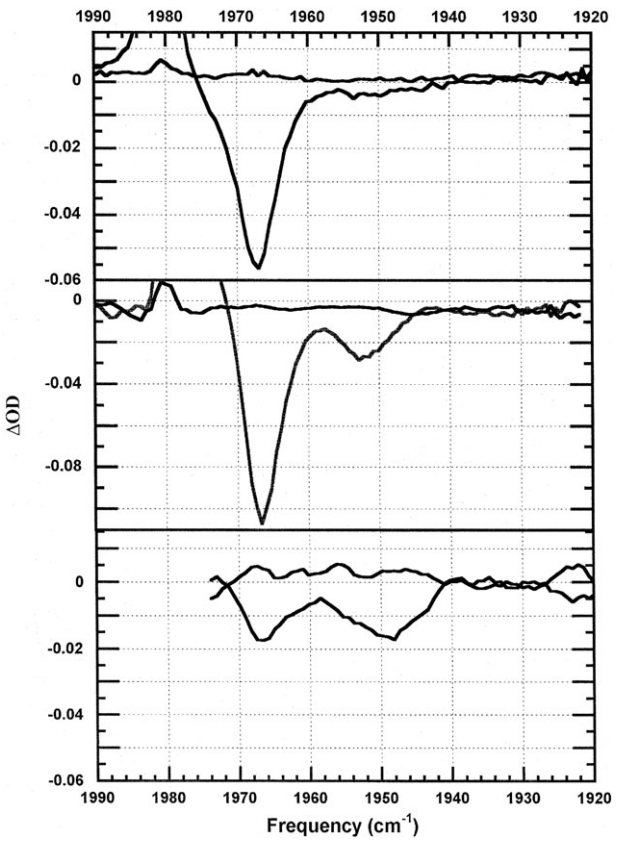

Fig. 12 Selective excitation of different vibrational levels.[229] Infrared transient difference spectra for $W(CO)^6$ in *n*-hexane at a probe delay time of 40 ps. The upper panel shows the result for positively chirped laser pulses, the middle for unchirped laser pulses and the lower for negatively chirped laser pulses centered near 1978 cm^{-1}. The signal of the $\nu = 1$ population is visible at 1967 cm^{-1} and the one of $\nu = 2$ at 1950 cm^{-1}. At 1982 cm^{-1}, the bleach of the $\nu = 0$ ground state is visible. From the three panels, it is clearly visible that negatively chirped laser pulses can efficiently populate the $\nu = 2$ level, while positively chirped laser pulses discriminate against it. Reprinted from *Chem. Phys.*, **233**, V. D. Kleiman, S. M. Arrivo, J. S. Melinger and E. J. Heilweil, Controlling condensed-phase vibrational excitation with tailored infrared pulses, 207–216, Copyright 1998, with permission from Elsevier and from the authors.

It has been shown for experiments in the gas phase that this ladder-climbing process can lead to dissociation of the molecules.[239] As already indicated in the experiments by Heilweil,[229] and also in the gas phase experiment presented in ref. 239, negatively chirped laser pulses have a higher dissociation yield than unchirped or positively chirped laser pulses. It is assumed that in the case of the molecule studied by the group of Heilweil, population of the levels higher than $\nu = 7$ leads to dissociation of the system.[240] Recently Motzkus and coworkers have shown that the population of the $\nu = 6$ vibrational level is possible for $W(CO)_6$ in the liquid phase by using femtosecond laser pulses whose spectrum covers the associated transition energies and whose peak intensity is high enough to allow population of the high levels.[240] Although dissociation by directly influencing the ground state dynamics has not yet been demonstrated in the liquid phase, the presented experiments are very encouraging with respect to this possibility.

These discussed examples of chirp control of different quantum mechanical systems show the essential influence of the spectral phase on the ensuing dynamics. Population transfer, wave packet motion and the excitation of vibrations have been shown to depend crucially on the linear chirp of the exciting laser pulse. Other applications such as improving the resolution of CARS experiments also take advantage of chirped laser pulses.

The presented experiments on wave packet focusing using chirped laser pulses visualize, among others, the dependence of the excited state dynamics on the phase of the excitation laser pulse. It can be seen that the behavior of the wave packet seriously affects the reaction outcome. Controlling the wave packet motion can therefore optimize the kinetics of the molecular system.

Using more sophisticated spectral phase functions will open up a more complex control of the dynamics. Such phase functions can be realized with the multiparameter control schemes presented in the next section. Several experiments discussed there demonstrate the influence of the phase to given control problems and prove the high potential of multiparameter control approaches to control the outcome of reactions even in the condensed phase.

IV. Multiparameter control

After the first multiparameter control experiments using a closed learning loop by the groups of Wilson,[58] Silberberg[8] and Gerber,[9] a growing number of experiments have been published on this topic for gas phase and also for condensed phase systems.

For better structuring, this section will be divided into different categories. Selective electronic excitation is treated first because influencing the fluorescence yield is the most common control objective.[58,104–108,110–114,119,129,241–243] The second subsection deals with several experiments that provide methods to influence the vibrational dynamics of a system. Finally the last subsection will present experiments with complex reaction types, especially on the topics of energy flow and molecular isomerization.

A. Selective electronic excitation

The very first adaptive femtosecond quantum control experiment has already been performed on a rather complex dye molecule in the liquid phase.[58] The control objective was maximization of the ratio of the fluorescence to the laser pulse energy on the one hand and the enhancement of the fluorescence yield in total on the other hand. Five laser pulse parameters could be altered using a genetic algorithm in order to achieve an optimal result, namely amplitude, second- and third-order spectral phase, the center frequency, and the spectral width of the laser pulse. For the first objective the determined laser pulse was shifted to the absorption maximum of the molecule and had a narrow spectrum. This ensures a high number of excited molecules and therefore a high fluorescence yield in relation to the laser pulse energy. The second control objective of maximizing the total fluorescence results in a strongly positively chirped laser pulse covering a broad spectral range. This laser pulse was 1.3 times as efficient as a transform-limited laser pulse. The control mechanisms can be explained by intrapulse dumping as shown in the experiments in section III D.

In case of very broad (inhomogeneous) lines, the full SFG region of the SOPS (Fig. 7, fourth column) can contribute to a two-photon excitation. One can see from Fig. 7 that for all spectral phases the SOPS never exceeds the one for a bandwidth-limited pulse, which hence excites best. This intensity dependence inheres in multiphoton excitation of very broad lines, and thus prevents gathering information about the system from adaptive pulse-shaping experiments, since only the trivial solution of a bandwidth-limited pulse is obtained (see also section III B). Our group showed that this intensity dependence can be circumvented by using the ratio of the two-photon induced emission to the SHG yield as control objective.[108] SHG is an intensity-dependent effect and can be thus used as a ''reference signal''. The successful control of the emission : SHG ratio demands pulse shapes that are adapted to the electronic structure or the dynamic needs of the molecule in solution. To demonstrate this concept, we successfully maximized and minimized the emission : SHG ratio for the molecule $[Ru(dpb)_3](PF_6)_2$ ($Ru(4,4'$-diphenyl-$2,2'$-bipyridine$)_3(PF_6)_2$) dissolved in methanol (see Fig. 13a). This molecule can be excited *via* two 800 nm photons. After nonradiative transfer from the initially populated ^{1}MLCT (metal-to-ligand charge transfer) state to the ^{3}MLCT state, the ground state is populated by emitting a photon (see Fig. 13b). This emission *versus* the SHG can then be used as feedback signal. To visualize the full data set, a scatter plot with the SHG on the *x*-axis and the emission on the *y*-axis has proven to be very helpful (Fig. 13c and d). In the case of an emission-only optimization, the emission yield is strictly correlated with the SHG outcome for the same pulses, and hence the tested pulse shapes from the optimization are grouped around a line with a slope of 1 in the scatter plot of Fig. 13d and e. In the case of the minimization and maximization of the emission : SHG ratio, two separate distributions of data points can be observed in the respective scatter plot (Fig. 13c). This indicates that due to the control objective, the learning algorithm evaluates pulse shapes in distinct regions of the variable

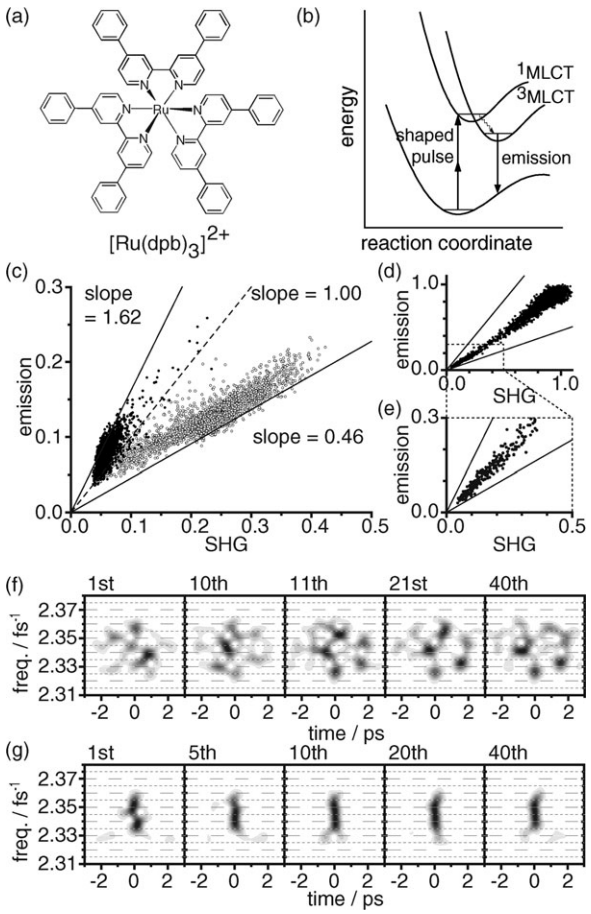

Fig. 13 (a) Drawing of the metal-to-ligand charge transfer (MLCT) chromophore. (b) Scheme of the multiphoton control methodology. The ^{1}MLCT band is excited *via* two photons. The emission from the lower ^{3}MLCT state is used as a feedback signal. (c) Removing the intensity dependence in the control of two-photon electronic excitation. The molecular system was $Ru(4,4'$-diphenyl-$2,2'$-bipyridine$)^3(PF_6)_2$ in methanol. (c) Scatter plot of the emission *vs.* SHG. The values from an adaptive maximization (solid circles) and a minimization (open circles) of the emission : SHG ratio are plotted. The solid lines have a slope reflecting the ratio of the best pulse from either of the two optimizations. The dashed line represents the ratios for unshaped pulses. (d) Values taken for the two observables from an emission-only maximization. (e) Subset of the emission-only maximization values, for the same range as in (c). (f) Evolution of the fittest pulse shape after different generations in the Husimi representation during the emission *vs.* SHG maximization (fittest laser pulses of generations 1, 10, 21, and 40). (g) Evolution during the emission *vs.* SHG minimization (fittest laser pulses of generations 1, 10, 20, and 40).[108]

space. The two lines with the slopes 0.46 and 1.62 mark the minimum and the maximum ratio achieved by pulses found in the respective optimizations. In comparison with the emission-only optimization, the scatter plot visualizes the successful removal of the intensity dependence by the chosen control objective. Because of the chosen control objective, the evolutionary algorithm has to find pulse shapes which are adapted to the electronic structure and molecular needs. The formation of such pulse shapes is illustrated in Fig. 13f for the case of the emission : SHG maximization and in Fig. 13g for the emission

: SHG minimization, respectively. In the maximization case, one can see that certain features are common in the fittest pulse shapes from different generations. These features are further adjusted in later generations and play a specific and important role in the excitation process. In the minimization case, the pulses found during the optimization are less structured than for the maximization. A comparison reveals that frequency components below 2.335 fs^{-1} lack significant intensity for the minimization, while distinct features in this regime are observed for the maximization. Thus, optimal pulse shapes and their evolution may provide insight into the underlying control mechanisms, that can be further studied by additional experiments, for example by reducing the problem complexity using parameterized scans (see for example the excitation of α-perylene at the end of this subsection).

Based on this optimization of two-photon excitation *versus* SHG, our group then investigated the possibility to selectively excite either of two different types of dye molecules in solution by two-photon absorption with shaped laser pulses.[105] The two molecules considered here were $[Ru(dpb)_3](PF_6)_2$ and DCM (4-dicyanomethylene-2-methyl-6-*p*-dimethylaminostyryl-4*H*-pyran). Again the measurement of spontaneous emission provided an indicator for the fraction of excited molecules of each type. The challenge in this case was that both molecules exhibit the same spectral behavior in their absorption profiles within the accessible range, so that wavelength-selective excitation does not work. The question here was whether it is possible to selectively excite one type of molecule with respect to another even if they have identical absorption spectra. The route to success lies in quantum control schemes that exploit specific wave packet propagation after the initial Franck–Condon transition. This propagation can be different for the two molecules.

For comparison, several single-parameter scans were performed first. For unshaped laser pulses, the ratio of the two-photon ground state absorption of the two molecules does not change over the bandwidth accessible with the laser system used (Fig. 14c). Therefore, using unshaped laser pulses, both molecules will fluoresce to a certain amount and changing the absorption wavelength will not change this situation significantly. Also, varying the second-order spectral phase from $-20\,000$ to $+20\,000$ fs^2 (Fig. 14b) or changing the laser pulse energy from 50 to 250 μJ (Fig. 14a) does not affect the emission ratio. The individual transition probabilities for the two molecules vary, but vary exactly in the same way (*e.g.* more intensity, more excitation) for both types, so the ratio remains constant. In contrast, with the help of adaptive femtosecond multiparameter control, it is possible to determine a laser pulse shape that changes this ratio by a factor of 1.5 (Fig. 14d) and hence increases the excitation probability selectively for one species. Since the initial Franck–Condon transition properties are identical for both systems (Fig. 14a–c), the control mechanism has to be based on the laser pulse interaction with the excited state wave packet after the initial excitation step. As the single parameter control mechanisms could not change the fitness significantly, a non-trivial coherent manipulation of excited state photophysics is a likely control mechanism. This experiment demonstrated the possibility of selective two-photon excitation even for molecules with similar one-photon and two-photon absorption spectra.[79,105,244] Such a selective two-photon excitation in the condensed phase achieved by coherent control techniques has a variety of applications in spectroscopy and microscopy. In recent years, several groups have demonstrated its applicability,[105–108,129,242,245–250] *e.g.* Dantus and coworkers who performed selective two-photon excitation of molecules

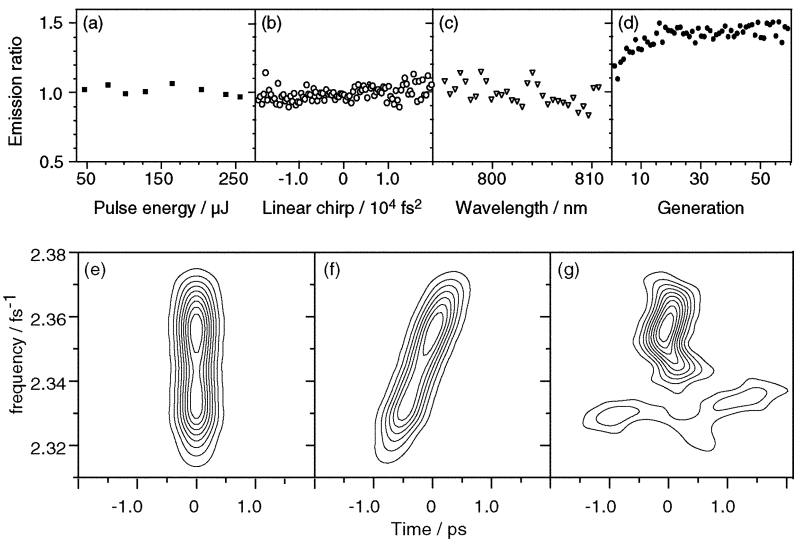

Fig. 14 Photoselective molecular excitation: Emission ratio of DCM (4-dicyanomethylene-2-methyl-6-*p*-dimethylaminostyryl-4*H*-pyran) *versus* Ru(4,4′-diphenyl-2,2′-bipyridine)$_3$$(PF_6)_2$ for different quantum control schemes. Both dye molecules are dissolved in methanol. (a) Emission ratio dependence on the laser pulse energy of the unshaped excitation laser pulse; (b) variation of the linear chirp; (c) scanning of a symmetric and rectangular spectral window of 5 nm width over the laser spectrum; (d) adaptive multiparameter optimization curve. Husimi representation of different pulse shapes used in the experiment: (e) unshaped laser pulse; (f) linear chirp of 2×10^4 fs^2; (g) the optimized electric field from the last generation of (d).[105]

through scattering biological tissue[246,247,250] or depending on the pH value of the environment.[242,245] Such optimized laser pulses as determined in our experiment could be helpful in two-photon excited fluorescence microscopy in the case of chromophores that have identical or near-identical two-photon spectra. Fig. 14e–g show the experimental Husimi representations for different laser pulse shapes. Fig. 14e represents the Husimi trace for a bandwidth-limited pulse and Fig. 14f the Husimi trace for an exemplary linearly chirped pulse, as used in the chirp scan. The shape of the optimized pulse is shown in Fig. 14g.

Very recently a nice experiment has been published that investigates the two-photon excitation efficiency of α-perylene crystals on the one hand and perylene in chloroform solution on the other.[113,114] To measure the two-photon excitation efficiency, the fluorescence signal was again recorded. Interestingly, for both states of aggregation, very similar laser pulse shapes have been the optimal solution to the given problem, showing a characteristic laser pulse train. The optimized laser pulses, obtained from the crystal experiment, even enhanced the fluorescence in the solution experiment and *vice versa*. Additional double-pulse experiments were carried out. In Fig. 15a the relative phase between the individual laser subpulses is scanned for a pulse separation of 90 fs and in Fig. 15b the laser pulse separation ("pulse interval"[113]) is varied for two fixed values of the relative phase difference of the individual subpulses. The plots show the dependence of the fluorescence intensity on the different parameters and confirm the findings of the feedback experiment for the case of the measurement in chloroform. From the similarity of the laser pulse shapes for the crystal and the solution experiment one can conclude that intramolecular processes play a major role in the control mechanism. In contrast to the electronic coherence, the vibrational coherence lasts longer than 1 ps in the investigated systems. The revealed laser pulse interval matches the period of vibrational motion that is strongly coupled with the electronic transition. Because of these reasons, the coherent excitation of vibronic states is thought to control the intramolecular vibrational-energy redistribution pathway and is responsible for the excitation efficiency increase.

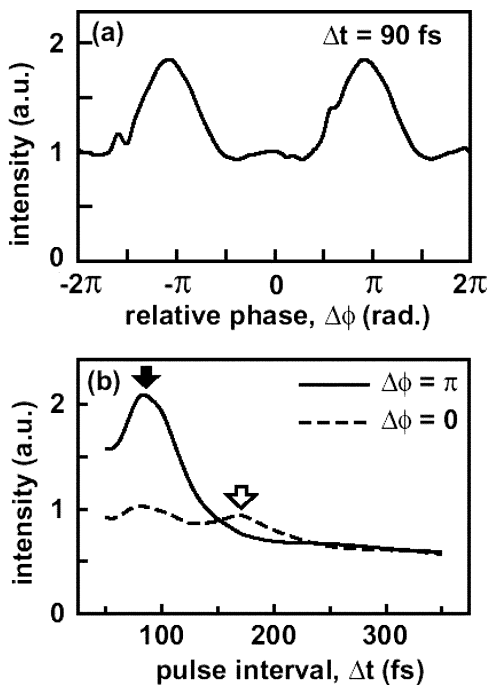

Fig. 15 Control of excitation efficiency in α-perylene and perylene in chloroform. Verification of the result found by adaptive femtosecond quantum control. The closed-loop multiparameter approach results in a laser pulse train. The above graphs show the dependence of the crystal fluorescence on (a) the relative phase between two laser pulses separated by 90 fs and (b) the laser pulse separation for two different relative phase values between the two individual laser pulses. Reprinted from ref. 113 with permission from the authors and the American Institute of Physics. Copyright 2004 American Institute of Physics.

The latter experiment can be interpreted in the context of a seminal experiment by Weiner *et al.*,[251] who have also used α-perylene crystals, but concentrated on the selective excitation of a certain vibrational mode. While in this subsection we have exemplified the power of pulse shaping for controlling electronic transitions, the next subsection addresses its potential for vibrational spectroscopy.

B. Control of vibrational excitation

In coherent vibrational spectroscopy, optimization experiments are normally not performed *via* shaped MIR electric fields, as laser pulse shaping in the MIR is hard to accomplish (though this is likely to change in the near future with the recent development of direct MIR pulse shaping by Zanni and coworkers[212]). Nevertheless, several technological realizations have been developed[205–212] and have been used to study chemical reactions in the liquid phase. For instance, as already mentioned, the group of Heilweil has employed chirped MIR laser pulses to study ladder climbing in liquid $W(CO)_6$ (Fig. 12),[229] and the group of Martin and Joffre performed ladder climbing in carboxyhemoglobin.[252] Tan and Warren used shaped MIR laser pulse sequences to measure the optical free-induction decay of the C–H stretching mode in liquid chloroform.[209]

Another method used to reveal the information contained in vibrational spectra is Raman spectroscopy in its many variations. As early as 1990, Weiner, Nelson and coworkers[251] have demonstrated mode-selective impulsive stimulated Raman scattering from molecules in an organic crystal with adapted excitation laser pulse shapes. They modulated the spectral phase so that a laser pulse train emerged with a distinct laser pulse spacing that matched the vibrational period of the desired mode. This mode could be repetitively driven by the laser pulse train, while the timing was ineffective for other modes (see Fig. 7, third column). Thus, both selective excitation and enhancement of a certain vibration were demonstrated.[251,253,254]

In 1999, Weinacht *et al.*[255] performed an adaptive control experiment on stimulated Raman scattering in liquid methanol. Since the Stokes shift was 30 times larger than the laser bandwidth, the mechanism was not impulsive as in the previously discussed experiment by Weiner *et al.* Thus, phase-shaped intense laser pulses were used that led to self-phase modulation (SPM) in the methanol sample, resulting in a

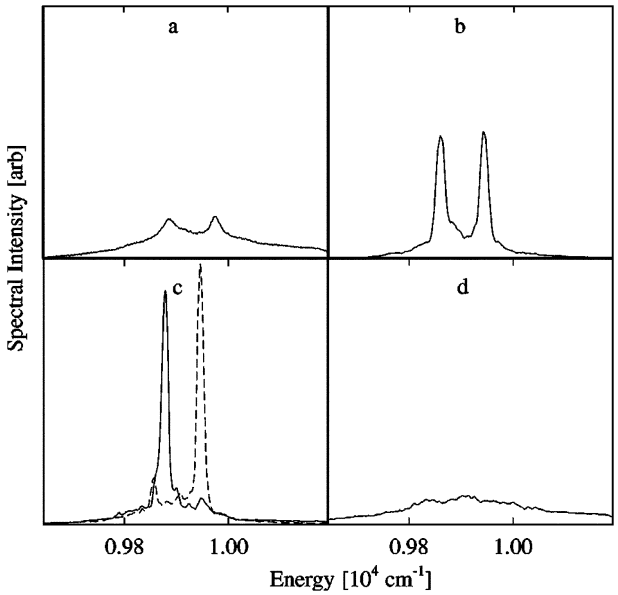

Fig. 16 Control of Raman scattering in methanol.[255] Forward scattered spectra for (a) an unshaped laser pulse, (b) a laser pulse optimizing the total Raman signal while minimizing peak broadening due to other nonlinear effects, (c) a laser pulse optimizing each mode independently, and (d) a laser pulse optimized to suppress the Raman scattering. Reprinted from T. C. Weinacht, J. L. White and P. H. Bucksbaum, *J. Phys. Chem. A*, 1999, **103**, 10166, with permission from the authors and the American Chemical Society. Copyright 1999 American Chemical Society.

spectral broadening (up to white-light generation), which could principally serve as a stimulated Stokes laser pulse. In a closed-loop learning control experiment, they were able to gain control and selectivity over the two spectral signatures (Stokes emission) of the symmetric and the asymmetric C–H stretch modes, and enhance or reduce both of them simultaneously. Fig. 16a shows the forward scattered spectrum for an unshaped laser pulse. In Fig. 16b the spectrum is presented for the case of optimizing the total signal while the peak broadening due to other nonlinear effects is minimized. The fact that either of the two peaks can be optimized separately is shown in Fig. 16c, and Fig. 16d shows the spectrum for the control objective of suppressing both of them. In subsequent experiments[14,15] on methanol and on C_6H_6 and C_6D_6, they concluded that the control mechanism is an intramolecular process, based on coupling between the two modes inside each molecule, rather than shaping the SPM in order to predominantly seed one mode. Furthermore, the optimal laser pulse consisted of a laser pulse sequence whose separation matched the beat frequency of the two modes. This indicated that the control could have been realized *via* a quasi-impulsive process where a beat of the two modes is initially excited and the energy could afterwards be redistributed impulsively.

These studies represent liquid-phase experiments in which the special challenges of condensed-phase control become apparent. A direct interpretation is very difficult due to the multitude of processes. SPM of the pulse in the medium is predominantly a third-order process that strongly depends on the pulse shape. The controlled spectral signatures of the Stokes emission are of third-order, too. This may result in a competing interplay so that these signatures are not directly reflecting the populations of the two vibrational modes any more, as Spanner and Brumer have shown in a theoretical study.[256,257] Their study also showed that these competing nonlinear effects allow control over the Stokes emission by variation of single pulse parameters without the need for a coherent quantum interference effect in the sample.

A widely used method for nonlinear spectroscopy is CARS. In this scheme, a pump (ω_{pu}), a Stokes (ω_S) and a probe (ω_{pr}) beam are employed in order to generate the anti-Stokes signal at $\omega_{aS} = \omega_{pu} - \omega_S + \omega_{pr}$. When the difference frequency $\omega_{pu} - \omega_S$ coincides with the energy of a vibrational level of the molecule under study, an enhanced anti-Stokes signal due to this resonance can be observed. With femtosecond laser pulses, it is possible to measure the transient behavior of the induced ground state dynamics, but there are also two major disadvantages. First, the large bandwidth of the laser pulses employed in most cases leads to excitation of several modes simultaneously and to a relatively low spectral resolution. Second, the short time duration and thus the high peak intensity leads to strong nonresonant background contributions.

In liquid phase multipulse CARS, *i.e.* where two or more laser pulses are employed, many different techniques have been developed that utilize one or more tailored femtosecond laser pulses in order to overcome at least one of these disadvantages. Even very simple control schemes, for which no pulse shaper is necessary, lead to an improvement. For example, one can already succeed by simply introducing linear chirp in order to enhance the spectral resolution and achieve limited mode selectivity.[233–235,258] More sophisticated approaches make use of the coherent properties of distinct laser pulse shapes by introducing coherent control schemes with pulse shapers.[259,260] Again, also in CARS the closed-loop approach has been applied, through which the electric field can be optimally adapted to the given molecular system. Materny and coworkers have demonstrated the usefulness of this multidimensional adaptation of the excitation step in condensed phase femtosecond CARS spectroscopy. Among the controlled processes are mode-selective excitation and suppression of certain modes.[258,261–263] The method has also provided a handle on the mode decay times and on the relative phases between vibrational modes.

As the spectral width of femtosecond lasers can span several vibrational levels, a single laser pulse in combination with a pulse shaper is sufficient to obtain high-resolution CARS spectra and coherently influence the excitation. This field has been pioneered by Silberberg and coworkers[181,183,264–266] who have introduced several different schemes since 2002 and applied them to CARS spectroscopy and microscopy. In analogy to the experiments by Weiner *et al.*[251,253,254] discussed earlier, the generation of laser pulse trains by imposing sinusoidal spectral phase patterns upon the laser pulse leads to selective excitation of a certain mode, while scanning the laser pulse spacing allows one to record Raman spectra.[183,264,266–269] Fig. 17 shows the results of this technique applied to three different organic substances. The insets visualize the derived Raman spectra from the CARS signal, plotted

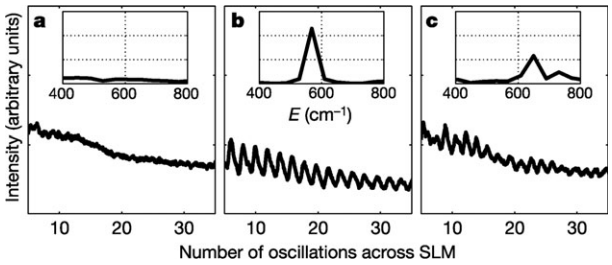

Fig. 17 Liquid phase single-pulse CARS spectroscopy of three organic substances.[264] As laser pulse trains are generated by different sinusoidal spectral phase patterns, the CARS signal is plotted as a function of the corresponding periods across the spatial light modulator (SLM). The derived Raman spectra are shown as inset. The three data sets correspond to (a) methanol (no resonance in the accessible frequency range), (b) CH_2Br_2 (one resonance), and (c) $(CH_2Cl)_2$ (two resonances), where the CARS signal shows a clear beating between the two accessible Raman modes. Reprinted with permission from the authors and from Macmillan Publishers Ltd: N. Dudovich, D. Oron and Y. Silberberg, *Nature*, 2002, **418**, 512, Copyright 2002.

as a function of the corresponding periods across the SLM. This can be easily visualized with the help of Fig. 7b. When the number of spectral phase oscillations across the spectrum is scanned (abscissae in Fig. 17), not only the temporal spacing of the created pulse train (Fig. 7b2) is varied, but also the modulation in the SOPS. A Raman transition corresponding to a frequency in the DFG region of the SOPS (Fig. 7b3) may therefore contribute strongly to the CARS signal (when the SOPS has a maximum at this frequency), while for another sinusoidal spectral phase it may not contribute at all (when the SOPS has a minimum). Fig. 17a shows the outcome of the measurements with methanol, which has no resonance in the accessible frequency range, Fig. 17b corresponds to CH_2Br_2, having one resonance, and Fig. 17c to $(CH_2Cl)_2$, with two resonances.

Due to the quantum control techniques the achievable spectral resolution, unmatched by conventional femtosecond CARS spectroscopy, is more than an order of magnitude better than the spectral width of the employed laser pulses. In another approach, only a small part of the laser pulse's spectrum is phase-shifted by the pulse shaper, which has an impact on the resonant CARS signal, and acts as an effective narrow probe. Thus, whole Raman spectra can be obtained from the interference of the resonant and the nonresonant contributions without having to scan any parameter.[265,266] In combination with polarization pulse-shaping first demonstrated in our group,[57,174–176] Silberberg's group has further improved this scheme to measure background-free CARS spectra with high spectral resolution.[181,183] Using this technique, they are also sensitive to the relative phase of excited modes. While one can already achieve a remarkable manipulation of condensed phase Raman spectra by simple schemes like linearly chirped[233–235,258] or differently polarized[270] excitation beams, it becomes clear from all the discussed implementations of pulse shaping that coherent control techniques have tremendously enriched the field of vibrational spectroscopy.

C. Control of energy flow and isomerization

In recent years, there has been an increasing interest in multiparameter control experiments dealing with biomolecular systems.[118,119,125,126,129,243] In 2002, the group of Motzkus published a study on the light-harvesting antenna complex LH2 from *Rhodopseudomonas acidophila*.[118] This system collects the sun light and makes the energy available to the reaction center. Part of the harvested light is transferred to a final acceptor state *via* two transition states while the rest is lost due to internal conversion. Both the internal conversion and the energy transfer process can be monitored by transient absorption spectroscopy. The corresponding transients are shown in Fig. 18. With the help of adaptive optimization in which 64 pulse-shaper pixels were independently varied, a pulse-train-like optimal laser pulse is obtained, which enhances the internal conversion process in relation to the energy transfer. Based on this finding, the group repeated the experiments using sinusoidal phase patterns which result in a pulse train whose spacing, modulation depth and phase differences can be influenced by three parameters. These experiments showed that pulse trains with a spacing of 250 fs efficiently increase the internal conversion. To demonstrate the coherence in the control mechanism, the parameter influencing the temporal phase between consecutive subpulses was scanned, which resulted in a modulation of the internal conversion to energy transfer ratio. Although it was not possible to increase the efficiency of the energy transfer beyond the limit given by nature, the experiment very nicely demonstrated the potential to influence reactions in complex biomolecular systems with tailored laser pulses. This experiment impressively demonstrated for the first time that biological systems can be coherently manipulated with tailored light pulses.

The first adaptive control of a liquid phase isomerization reaction was demonstrated in our group using the example of

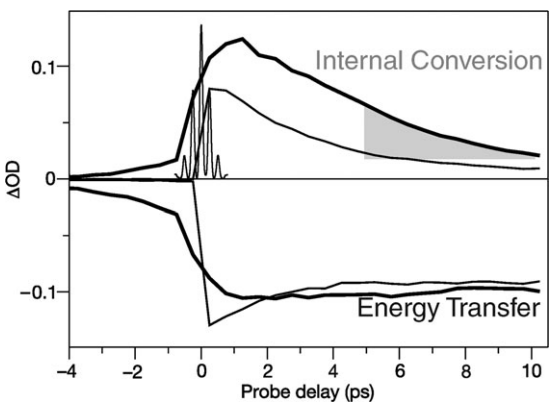

Fig. 18 Controlling the energy flow in LH2. The transient with positive absorption values visualizes the internal conversion process and the lower transient the energy transfer to the reaction center. Thin line: transform-limited excitation; thick line: transients for excitation with optimized laser pulses. A typical shaped laser pulse is sketched as well. As feedback for the internal conversion process the shaded region is taken and in the case of the energy transfer, the asymptotic signal. Adapted by permission from the authors and from Macmillan Publishers Ltd: J. L. Herek, W. Wohlleben, R. J. Cogdell, D. Zeidler and M. Motzkus, *Nature*, 2002, **417**, 533. Copyright 2002 (ref. 118).

a dye molecule dissolved in methanol.[109] This dye molecule (NK88) exists in the isomer forms *trans* and *cis*. At room temperature, only the *trans* isomer is present. After electronic excitation to S_1, the repopulation of the ground state can lead either to regions of the PESs corresponding to *cis* or back to the original *trans* configuration. The time-resolved pump–probe transient absorption spectra are shown in Fig. 19c for 400 nm pump pulses and probe wavelengths covering the complete visible range. Around 400 nm pump depletion occurs (Fig. 19a), while at 460 nm and at late delay times the absorption signals of the produced *cis* isomers can be monitored (Fig. 19b). At 500 nm stimulated emission is present, excited state absorption can be recorded at wavelengths around 360 nm, and also around 900 nm where stimulated emission takes place as well. A combined experimental and theoretical analysis suggested two-time dynamics on the excited state (2–3 ps and 9 ps) and a hot ground state absorption with a decay time of about 10 ps.[271,272] In order to detect the isomerization efficiency, the amount of produced *cis* isomers as well as the amount of excited molecules were measured by transient absorption spectroscopy. Changing the ratio of these two signals corresponds to influencing the isomerization efficiency, *i.e.* the quantum yield. As can be seen in Fig. 19 both enhancement (Fig. 19b) as well as reduction (Fig. 19c) of the isomerization efficiency could be achieved.

A theoretical study by Hoki and Brumer[273] investigated possible control mechanisms for a model isomerizing system similar to the molecule NK88. Their theoretical model comprises a one-dimensional motion plus decoherence by considering system–bath coupling, while it does not take into account excitation to other electronic states, multi-dimensional motion or nuclear vibrational modes. Nevertheless, the accordance of the simulated electric fields[273] with the experimental ones[109] is remarkable. Several theoretical studies have addressed the controllability of *cis–trans* isomerization in dye molecules, confirming its feasibility with femtosecond laser pulses. Among them are both calculations taking into account interactions with solvent molecules[273,274] and those considering isolated molecules.[274–277] The work by Hunt and Robb[277] suggests that controlling the initial momentum distribution of the wave packet on a multidimensional excited state PES is a means to influence the reaction outcome. Experimental evidence for such a scenario is discussed in a recent experiment by Yartsev and coworkers[278] who manipulated the absolute isomerization yield of the dye 1,1′-diethyl-2,2′-cyanine in solution by applying a closed-loop optimal control scheme.

Other theoretical works have also investigated how to control isomerization reactions, though mostly not in the condensed phase. A very prominent example studied in both

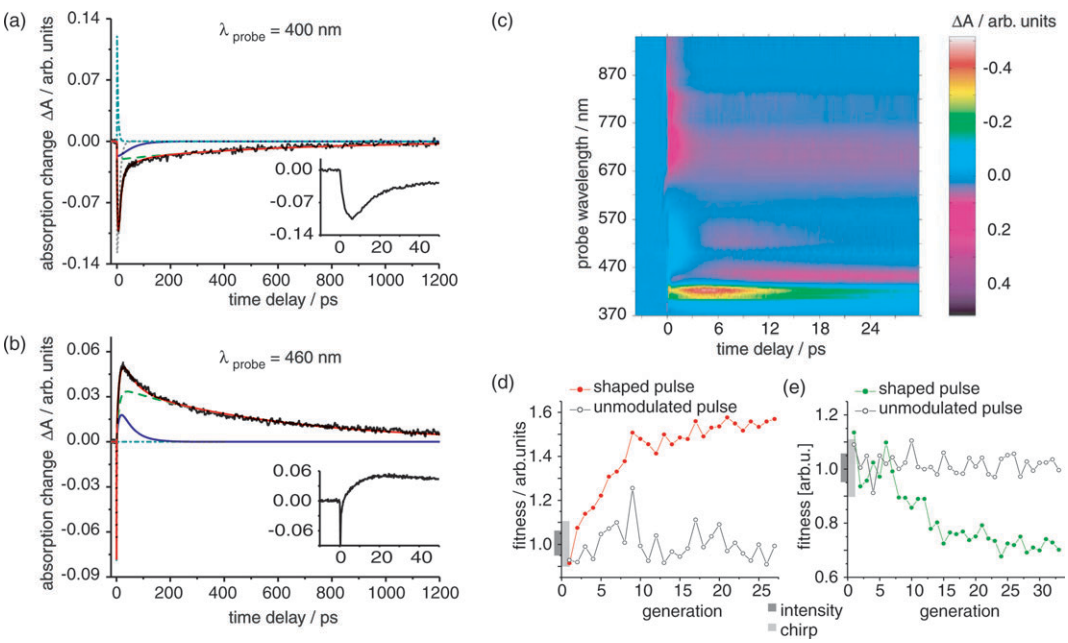

Fig. 19 Pump–probe transient absorption spectroscopy of the molecular dynamics of NK88 at a pump wavelength of 400 nm: Transient absorption signal at probe wavelengths of (a) 400 nm and (b) 460 nm. Black shows the experimental data points, while red marks fitted curves. The individual contributions to the fits are also shown to visualize the different time constants, while insets show the behavior of the transients during the first 50 ps. At 400 nm, pump-depletion is visible, while the absorption signal around 460 nm represents the amount of produced isomers. For more information and detailed modeling of the underlying processes see ref. 271 and 272. (c) Spectrally resolved transient absorption signal with probe wavelengths covering the spectral range from 370–950 nm. The *z*-axis (ΔA) of the contour plot describes the change in absorption of the probe beam. While red denotes a high transmission (decrease in absorption) through the sample, purple marks increased absorption of the probe beam. Control of photoisomerization efficiency of the molecule NK88: (d) maximization and (e) minimization of the *cis*/*trans* ratio as a function of generation using an evolutionary algorithm. The filled dots represent results obtained with shaped laser pulses (average of the ten best individuals). The open dots show the reference signal obtained with an unshaped laser pulse that is sent after each generation. On the fitness-axis the achievable ratios for the single-parameter control schemes of laser pulse energy (dark gray, 2σ width) and quadratic spectral phase (light gray) variation are also shown.[109]

the gas phase[279–285] and liquid environment[285,286] is the isomerization of the small molecule hydrogen cyanide. The controllability of very complex systems has also been investigated theoretically, *e.g.* for the retinal isomerization reactions in the proteins rhodopsin[287,288] and bacteriorhodopsin.[289]

The latter system, retinal in bacteriorhodopsin, has been chosen in a very recent experiment performed by Prokhorenko *et al.*[127] on the control of photoisomerization. At room temperature the thermodynamically most stable state has all-*trans* geometry. After irradiation with light, the system can isomerize to the 13-*cis* product state. The absorption of this product state is monitored at a wavelength around 630 nm. Using a closed-loop control scheme allowing both phase and amplitude shaping, the group succeeded in manipulating the amount of photoproducts by 20% in both directions. The absorbed number of photons of the optimized and the unshaped pulses were the same for all cases. Furthermore the experiments were performed in a regime where the response is linear with respect to the absorbed energy. Therefore the amount of excited molecules is equal for all three cases and therewith a change in the amount of products means a change of the isomerization efficiency.

Our group also worked on the control of the isomerization of retinal in bacteriorhodopsin, continuing our earlier work on NK88. However, we followed a different objective than that of the Prokhorenko *et al.* experiment and implemented control with shaped dump laser pulses. This pump-shaped-dump–probe scheme is an extension of the pump–dump work on retinal in bacteriorhodopsin by the groups of Anfinrud[115] and Ruhman[117] presented in section IIIC. In contrast to those conventional pump–dump schemes[115,117] and to experiments where the excitation pulse is shaped,[127] we have used a dump pulse whose spectral phase can be additionally shaped. Rather than aiming at optimal excitation we seek optimal de-excitation instead, as illustrated in Fig. 20a. An excited state wave packet induced by the pump pulse can be manipulated away from the initial Franck–Condon region, close to the conical intersection. Depending on the shape of the dump pulse and its temporal delay with respect to the pump, one can intervene in the evolution in the excited state.

In our experiment with bacteriorhodopsin, the system is excited to S_3 with 400 nm pulses, from where it descends to S_1. After evolution on S_1, part of the population is dumped back to the all-*trans* ground state by a near-infrared dump pulse before it can undergo isomerization to the 13-*cis* configuration. With the help of adaptive femtosecond quantum control, the best temporal delay and the best laser pulse shape for the dump pulse is determined. It turns out that within the spectral limitation of the laser system used, the pulse shape for most efficient dumping is given by a nearly transform-limited laser pulse delayed by 200 fs with respect to the pump pulse (Fig. 20c and d). Therefore with the help of a pump–dump scheme, the product isomer yield can be influenced. Using transient absorption spectroscopy, the effect of the pump–dump process on the isomerization reaction can be recorded. The evolution curve of this optimization with 128 free phase parameters is shown in Fig. 20c and the signal level for unmodulated dump pulses for a delay time of 200 fs is indicated by the dashed line.

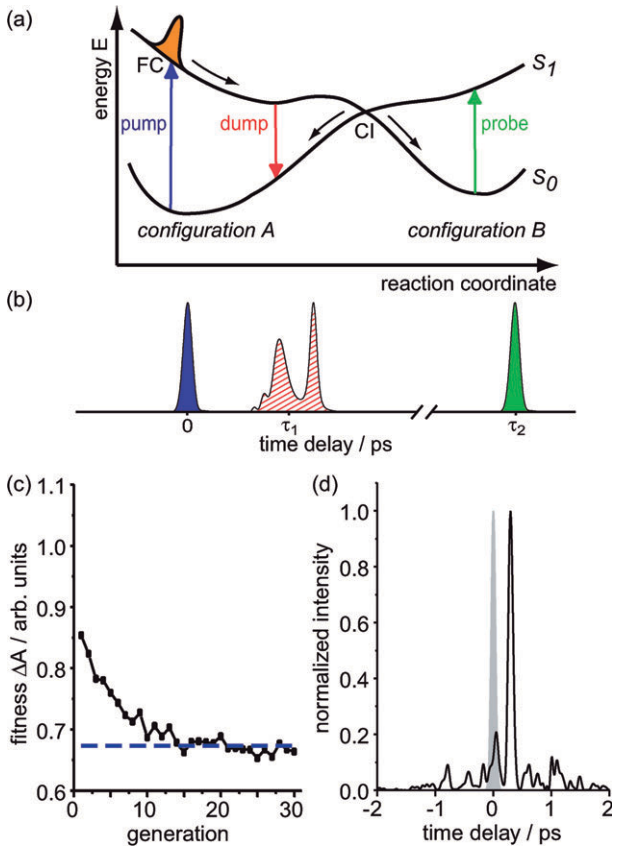

Fig. 20 (a) Sketch illustrating pump-shaped dump control: a PES for a typical molecule. After $S_0 \rightarrow S_1$ excitation by a pump pulse, the induced wave packet moves from the Franck–Condon region (FC) to the conical intersection (CI), where it can decay back to the S_0 PES. With a certain probability, either molecular configuration A or B is populated. An additional dump pulse can transfer population back to the ground state before the transition through the conical intersection occurs. (b) Pump-shaped dump–probe sequence. In this example, the shaped dump pulse (red hatched) is delayed by τ_1 with respect to the pump pulse (blue). The impact of the dump pulse, *i.e.* the final population in configuration B, is monitored by the probe pulse (green), which arrives at a time delay $\tau_2 \gg \tau_1$ after the pump pulse. (c) Pump-shaped dump control of retinal in bacteriorhodopsin. Evolution curve for optimizing the dumping effect. Each data point represents the average of the ten fittest individuals of one generation. The dashed line indicates the signal level of an unmodulated laser pulse with a linear spectral phase of 200 fs. (d) The resulting temporal intensity profile of the optimal 800 nm dump-laser pulse. The position of the 400 nm pump pulse is indicated in gray. Reprinted from *Chem. Phys. Lett.*, **433**, G. Vogt, P. Nuernberger, T. Brixner and G. Gerber, Femtosecond pump–shaped-dump quantum control of retinal isomerization in bacteriorhodopsin, pp. 211–215, Copyright 2006, with permission from Elsevier (ref. 128).

The pump-shaped dump approach has the potential to guide a wave packet during its propagation to the conical intersection at which it is transferred to the ground state. In general, the technique employing shaped dump pulses provides an additional efficient means to control complex systems with a broad spectral distribution of transitions. Furthermore, besides variation of the time delay between pump and dump pulses and adaptive determination of the optimal dump pulse,

the versatility of a femtosecond pulse shaper allows one to record systematic fitness landscapes as a function of selected pulse parameters, providing additional information on wave packet evolution and the PESs of the system under study.[290] Since the spectra of the dump and the pump pulse may be in different wavelength regions, the pump-shaped dump–probe scheme facilitates control of molecular systems away from the initial Franck–Condon window in regions of the PESs where the decisive reaction step occurs.

V. Summary and outlook

A. Current femtosecond condensed phase control

In recent years, many groups have developed and demonstrated a variety of different femtosecond optical control concepts applicable to condensed phase quantum systems. Numerous experiments and applications on a high number of different systems have been realized using these control methods and have shown their potential to influence molecular dynamics and chemical reaction outcomes in the condensed phase.

Single-parameter control schemes have proven to be able to influence condensed phase systems in various ways. Changing the excitation wavelength can influence the kinetics of the reaction, and the region of a PES where a wave packet is formed can be altered by scanning the excitation wavelength. Thereby even different electronic PESs can be addressed, changing significantly the successive dynamics as demonstrated for the case of dissociation of I_3^- into two or three fragments.

Wave packet dynamics in condensed phase systems can also be efficiently affected by pump–dump sequences, often a direct realization of the Tannor–Kosloff–Rice scheme. Various experiments have shown that many control objectives can be satisfied with pump–dump sequences, for example influencing isomerization dynamics or the population of a certain state to a desired time.

In a multitude of experiments the influence of chirped excitation pulses has been investigated. Chirping the pump laser pulse can be used to alter the amount of excited molecules, furthermore selective excitation of wave packet motion and wave packet focusing have been realized. This can be a very useful mechanism for the control of an intermediate step in order to alter reaction dynamics at a later time. Besides these applications of chirped laser pulses, they have also been used to selectively excite different vibrational modes. This can be seen as a first step in controlling reactions on the ground state PES.

These single-parameter control schemes have demonstrated that it is possible to control many quantum mechanical condensed phase systems in various ways. The development of pulse-shaping techniques made it possible to realize more complex control schemes.

First experiments employing such pulse-shaping techniques have been applied to the condensed phase for problems dealing with the excitation efficiency of quantum systems. The enhancement of the fluorescence efficiency or the selective excitation of dye molecules have been among the early multi-parameter control goals in liquids, having direct applications in two-photon microscopy, *e.g.* to increase the image contrast or to single out certain features.

Also in the field of Raman spectroscopy, multiparameter schemes are successfully applied to different control objectives. For instance, it is possible to control stimulated Raman scattering and to selectively excite different vibrational modes. Furthermore pulse shaping is used for different applications in CARS. The use of pulse-shaping techniques can help to reduce the number of necessary laser beams for CARS to only one beam without losing the temporal information accessible with ultrashort pulses. Several experiments have been published which make use of shaped pulses to improve the spectral resolution of multi-beam CARS experiments. In combination with polarization pulse shaping it was possible to measure background-free CARS spectra with high spectral resolution.

Important experimental steps have been taken towards the control of more complicated reactions in condensed phase systems with the control of energy flow in a complex biological system and the control of *cis–trans* photoisomerization dynamics. These experiments have shown that the concept of optimal control is applicable to such reaction types and large organic quantum systems. However, there are many reaction types and topics where a lot of work still needs to be done and that offer exciting opportunities for future optimal control experiments in the condensed phase, as will be discussed in the following.

B. Control of bimolecular reactions

Bimolecular reactions are necessary for molecular synthesis. The liquid environment has traditionally been essential for synthetic chemistry, because there, due to the high particle density, bimolecular reactions are very efficient. Laser-assisted bond cleavage within bimolecular reactions and the formation of large molecules from smaller fragments have been of great interest since the early 1980s. This way to form new molecules has been investigated in the gas phase[38,291–299] and liquid phase,[300–310] the natural environment for such reactions. The formation of bonds can be roughly divided into two different categories: the excitation of a free-to-bound transition (*e.g.* ref. 294, 296, 299) and bond activation (*e.g.* ref. 307, 308, 311). The first category can for instance be realized if the reaction partners are initially in a weakly bound electronic ground state, which is for example the case if they are part of a van der Waals precursor.[294,299] But initially unbound reaction partners have also experimentally proven to be able to perform a photoassociation process.[38,296] Moreover, the group of Zewail has shown that it is possible to influence the reaction outcome of such a photoassociation process in the gas phase with the help of a pump–repump scheme.[38]

While most experiments on free-to-bound transitions are performed in the gas phase, in the liquid phase a harpoon-type bond formation has been observed for Cl_2 dissolved in liquid Xe.[302] The final product, $Xe^+Cl_2^-$ is formed within 330 fs and the transition state Xe^+Cl^- even faster.

Bond activation of organometallic compounds has been intensively investigated by the group of Harris.[307,308] After dissociation of the compound, different excited transition

states can be populated and bond formation with a solvent molecule can finally occur. The time duration of such reactions in the liquid phase strongly depends on the solute and the solvent. Bond formation of photodissociated $Cr(CO)_6$ is reported to occur in less than one picosecond depending on the solvent.[300,305] In contrast, the appearance time of the bound product–complexes of other reactions can also be significantly longer, in the few tens[305,308] or even 100 ps time regime.[307] Nevertheless, the dissociation in general takes place on a subpicosecond timescale[4] and also the population of the succeeding transition states can occur significantly faster than the appearance time of the final reaction products.

Despite this extensive work on the observation of bond formation, the optical control of bimolecular reaction products in the condensed phase has not been demonstrated yet. However, bimolecular reactions based on free-to-bound transitions in the liquid phase should be able to be affected by specifically designed laser fields using similar mechanisms as in the gas phase, where it has been shown that the process of photoassociation can be controlled by two femtosecond laser pulses exhibiting a certain time delay.[38] In general though, there are very few experiments dealing with quantum control of gas phase bimolecular reactions. One of the reasons is that certain preparatory conditions have to be met in order to exploit interference effects in control experiments involving a reactive scattering process, as *e.g.* discussed in ref. 77, 90, 312. Therefore, controlling this type of reaction is generally a challenging task.

Very successful photoassociation experiments are performed in cold traps where laser-cooling techniques are employed. As the high vibrational levels accessed by photoassociation spectroscopy have a relatively small vibrational spacing compared to the spectral width of femtosecond lasers, the high number of synchronously excited vibrational levels will exacerbate coherent control of photoassociation with femtosecond lasers.[313] However, both theoretical[314–317] and first experimental studies[318–320] using tailored laser pulses in a cold trap have been performed recently for systems under such conditions. It will be interesting to see if/how the knowledge and experience from this field may be transferred to condensed phase photoassociation experiments.

C. Control of photodissociation

For bond formation based on bond activation, photodissociation or excitation to a higher level can be the first step. Many experiments have shown that it is possible to efficiently control the process of photodissociation in the gas phase.[59,61–65,67] In the condensed phase only simple control mechanisms have been demonstrated up to now, using different excitation wavelengths or varying the second-order spectral phase of the excitation laser pulse (see sections IIIA and IIID). Using a multiparameter control approach to control the population of different dissociation channels has not been demonstrated yet for condensed phase systems. Since the reaction timescale on which such photodissociation processes take place is very fast, there is no reason why such processes should not be controllable in the condensed phase. If the system is chosen in a way that the triggered photodissociation is the initial step for a bond activation, the subsequent bond-formation processes will automatically lead to the desired products, depending on the initial photodissociation fragments. The selective control of dissociation reactions in the condensed phase is a very interesting field for future experiments.

D. Control of stereoselectivity

A further field in which adaptive femtosecond quantum control can provide the necessary concepts is stereoselectivity. For example, the selective control of enantiomer concentration in initially racemic mixtures is an important application in chemistry. Naturally, the liquid phase is the most suitable environment for high product yields. Ultrafast feedback signals can be provided by measuring the optical activity. Due to the high relevance of selective control of enantiomer concentrations, several approaches have been developed theoretically[130–143] often incorporating the influence of the polarization of the light. Although first experiments without complex pulse shaping techniques have been conducted on this topic,[144,145] efficient conversion under standard laboratory conditions has not been demonstrated yet. With the recent advances in shaping the polarization,[57,174–187] adaptive femtosecond quantum control could provide the key concepts to achieve selectivity of enantiomers.

E. Control of molecular switching processes

Another application in ultrafast spectroscopy that recently gained a lot of attention is using molecules as switches. Molecular switches are especially interesting because of their scale and cost. Switching between different conditions is required for many applications such as data storage.[321] For reliable applications it is necessary to switch efficiently between the different states, which can be accomplished by adaptive femtosecond quantum control methods. In recent years, several groups of molecular switches have been developed, incorporating a huge number of molecules.[321] The switching process itself results in the rearrangement of many atoms, often grouped in rings or chains. Therefore the timescale for the switching can be in the millisecond regime or even longer. Such complicated rearrangement processes are difficult to control directly by optimal control methods. Nevertheless, they are often initiated by a reaction of a small part of the whole system, as it is for example in the case for retinal in bacteriorhodopsin. There, the isomerization reaction of the molecule retinal, which takes place on the femtosecond to picosecond timescale, triggers the photocycle of the protein, which itself lasts for several milliseconds.[322] Having an impact on the initial dynamics of the molecule retinal will finally control the photocycle. As shown in the discussed experiments, adaptive femtosecond quantum control can provide the means necessary to control switching reactions under such conditions. These successful experiments encourage further research on controlling the switching behavior of both small and complex systems with high efficiency.

F. Other applications and perspectives

Pulse shaping and quantum control are also appropriate methods for optical technology applications. Very recently,

manipulation of the two-photon induced birefringence in polymeric films could be demonstrated with shaped pulses.[323] This experiment is one example showing that a macroscopic effect, like absorptivity or birefringence, can be controlled, and not only the molecular properties on a pure microscopic scale.

Optimal control has proven to be a very successful concept for the control and investigation of many different types of quantum systems in various environments. The fundamental techniques for condensed phase systems are now well developed and have a high potential to provide solutions to many unsolved problems, like the control of reaction types outlined in the last paragraphs, and other relevant chemical, physical, and biological processes.

Acknowledgements

We thank our colleagues who gave us permission to use material from their publications. We have given an overview of femtosecond condensed phase quantum control, without the claim to cover every experiment ever conducted in this field. Nevertheless, we would like to apologize to those whose work might not have made it into our discussion.

PN acknowledges the support of the German National Academic Foundation (Studienstiftung des deutschen Volkes), and TB thanks the German Science Foundation for an Emmy Noether Fellowship.

References

1 N. Bloembergen and E. Yablonovitch, *Phys. Today*, 1978, **31**(5), 23.
2 A. H. Zewail, *Phys. Today*, 1980, **33**(11), 27.
3 N. Bloembergen and A. H. Zewail, *J. Phys. Chem.*, 1984, **88**, 5459.
4 A. H. Zewail, *J. Phys. Chem.*, 1996, **100**, 12701.
5 T. Elsaesser and W. Kaiser, *Annu. Rev. Phys. Chem.*, 1991, **42**, 83.
6 A. H. Zewail, *J. Phys. Chem. A*, 2000, **104**, 5660.
7 Y. Ohtsuki, K. Nakagami and Y. Fujimura, *J. Chem. Phys.*, 2001, **114**, 8867.
8 D. Yelin, D. Meshulach and Y. Silberberg, *Opt. Lett.*, 1997, **22**, 1793.
9 T. Baumert, T. Brixner, V. Seyfried, M. Strehle and G. Gerber, *Appl. Phys. B*, 1997, **65**, 779.
10 T. Brixner, M. Strehle and G. Gerber, *Appl. Phys. B*, 1999, **68**, 281.
11 T. Brixner, A. Oehrlein, M. Strehle and G. Gerber, *Appl. Phys. B*, 2000, **70**, S119.
12 D. Zeidler, T. Hornung, D. Proch and M. Motzkus, *Appl. Phys. B*, 2000, **70**, S125.
13 E. Zeek, R. Bartels, M. M. Murnane, H. C. Kapteyn, S. Backus and G. Vdovin, *Opt. Lett.*, 2000, **25**, 587.
14 B. J. Pearson, J. L. White, T. C. Weinacht and P. H. Bucksbaum, *Phys. Rev. A*, 2001, **63**, 063412.
15 T. C. Weinacht and P. H. Bucksbaum, *J. Opt. B*, 2002, **4**, R35.
16 F. L. Légaré, J. M. Fraser, D. M. Villeneuve and P. B. Corkum, *Appl. Phys. B*, 2002, **74**, S279.
17 T. Pfeifer, U. Weichmann, S. Zipfel and G. Gerber, *J. Mod. Opt.*, 2003, **50**, 705.
18 V. V. Lozovoy, I. Pastirk and M. Dantus, *Opt. Lett.*, 2004, **29**, 775.
19 K.-H. Hong and C. H. Nam, *Jpn. J. Appl. Phys.*, 2004, **43**, 5289.
20 A. P. Heberle, J. J. Baumberg, T. Kuhn and K. Köhler, *Physica B*, 1999, **272**, 360–362.
21 J. Kunde, B. Baumann, S. Arlt, F. Morier-Genoud, U. Siegner and U. Keller, *Appl. Phys. Lett.*, 2000, **77**, 924.
22 J. Kunde, B. Baumann, S. Arlt, F. Morier-Genoud, U. Siegner and U. Keller, *J. Opt. Soc. Am. B*, 2001, **18**, 872.
23 R. M. Koehl and K. A. Nelson, *J. Chem. Phys.*, 2001, **114**, 1443.
24 R. M. Koehl and K. A. Nelson, *Chem. Phys.*, 2001, **267**, 151–159.
25 Y. Toda, T. Nakaoka, R. Morita, M. Yamashita, T. Inoue and Y. Arakawa, *Physica E*, 2004, **21**, 180.
26 R. Fanciulli, A. M. Weiner, M. M. Dignam, D. Meinhold and K. Leo, *Phys. Rev. B*, 2005, **71**, 153304.
27 J.-H. Chung and A. M. Weiner, *IEEE J. Quantum Electron.*, 2006, **12**, 297.
28 T. Feurer, J. C. Vaughan and K. A. Nelson, *Science*, 2003, **299**, 374.
29 P. Brumer and M. Shapiro, *Chem. Phys. Lett.*, 1986, **126**, 541–564.
30 M. Shapiro, J. W. Hepburn and P. Brumer, *Chem. Phys. Lett.*, 1988, **149**, 451–454.
31 C. Chen, Y.-Y. Yin and D. S. Elliott, *Phys. Rev. Lett.*, 1990, **64**, 507–510.
32 D. J. Tannor and S. A. Rice, *J. Chem. Phys.*, 1985, **83**, 5013.
33 D. J. Tannor, R. Kosloff and S. A. Rice, *J. Chem. Phys.*, 1986, **85**, 5805.
34 R. J. Gordon and S. A. Rice, *Annu. Rev. Phys. Chem.*, 1997, **48**, 601–641.
35 T. Baumert, M. Grosser, R. Thalweiser and G. Gerber, *Phys. Rev. Lett.*, 1991, **67**, 3753.
36 T. Baumert, B. Bühler, M. Grosser, R. Thalweiser, V. Weiss, E. Wiedenmann and G. Gerber, *J. Phys. Chem.*, 1991, **95**, 8103.
37 T. Baumert and G. Gerber, *Isr. J. Chem.*, 94, **34**, 103.
38 E. D. Potter, J. L. Herek, S. Petersen, Q. Liu and A. H. Zewail, *Nature*, 1992, **355**, 66.
39 K. Bergmann, H. Theuer and B. W. Shore, *Rev. Mod. Phys.*, 1998, **70**, 1003.
40 N. V. Vitanov, T. Halfmann, B. W. Shore and K. Bergmann, *Annu. Rev. Phys. Chem.*, 2001, **52**, 763–809.
41 M. M. T. Loy, *Phys. Rev. Lett.*, 1974, **32**, 814–817.
42 J. S. Melinger, S. R. Gandhi, A. Hariharan, J. X. Tull and W. S. Warren, *Phys. Rev. Lett.*, 1992, **68**, 2000–2003.
43 B. Broers, H. B. van Linden van den Heuvell and L. D. Noordam, *Phys. Rev. Lett.*, 1992, **69**, 2062–2065.
44 U. Gaubatz, P. Rudecki, M. Becker, S. Schiemann, M. Külz and K. Bergmann, *Chem. Phys. Lett.*, 1988, **149**, 463–468.
45 A. Shi, A. Woody and H. Rabitz, *J. Chem. Phys.*, 1988, **88**, 6870.
46 A. P. Peirce, M. Dahleh and H. Rabitz, *Phys. Rev. A*, 1988, **37**, 4950.
47 R. Kosloff, S. A. Rice, P. Gaspard, S. Tersigni and D. J. Tannor, *Chem. Phys.*, 1989, **139**, 201.
48 W. Jakubetz, J. Manz and H.-J. Schreier, *Chem. Phys. Lett.*, 1990, **165**, 100.
49 J. E. Combariza, B. Just, J. Manz and G. K. Paramonov, *J. Phys. Chem.*, 1991, **95**, 10351–10359.
50 M. Sugawara and Y. Fujimura, *J. Chem. Phys.*, 1994, **100**, 5646.
51 R. S. Judson and H. Rabitz, *Phys. Rev. Lett.*, 1992, **68**, 1500–1503.
52 A. M. Weiner, *Rev. Sci. Instrum.*, 2000, **71**, 1929.
53 D. Goswami, *Phys. Rep.*, 2003, **374**, 385.
54 A. M. Weiner, D. E. Leaird, J. S. Patel and J. R. Wullert, *Opt. Lett.*, 1990, **15**, 326.
55 M. M. Wefers and K. A. Nelson, *Opt. Lett.*, 1993, **18**, 2032.
56 C. W. Hillegas, J. X. Hull, D. Goswami, D. Strickland and W. S. Warren, *Opt. Lett.*, 1994, **19**, 737–739.
57 T. Brixner and G. Gerber, *Opt. Lett.*, 2001, **26**, 557.
58 C. J. Bardeen, V. V. Yakovlev, K. R. Wilson, S. D. Carpenter, P. M. Weber and W. S. Warren, *Chem. Phys. Lett.*, 1997, **280**, 151.
59 A. Assion, T. Baumert, M. Bergt, T. Brixner, B. Kiefer, V. Seyfried, M. Strehle and G. Gerber, *Science*, 1998, **282**, 919.
60 D. Meshulach and Y. Silberberg, *Nature*, 1998, **396**, 239.
61 M. Bergt, T. Brixner, B. Kiefer, M. Strehle and G. Gerber, *J. Phys. Chem. A*, 1999, **103**, 10381.
62 N. H. Damrauer, C. Dietl, G. Krampert, S. H. Lee, K. H. Jung and G. Gerber, *Eur. Phys. J. D*, 2002, **103**, 71.
63 Š. Vajda, A. Bartelt, E. Kaposta, T. Leisner, C. Lupulescu, S. Minemoto, P. Rosendo-Francisco and L. Wöste, *Chem. Phys.*, 2001, **267**, 231.
64 R. J. Levis, G. M. Menkir and H. Rabitz, *Science*, 2001, **292**, 709.
65 C. Daniel, J. Full, L. González, C. Lupulescu, J. Manz, A. Merli, Š. Vajda and L. Wöste, *Science*, 2003, **299**, 536.

66 E. Papastathopoulos, M. Strehle and G. Gerber, *Chem. Phys. Lett*., 2005, **408**, 65.
67 D. Cardoza, C. Trallero-Herrero, F. Langhojer, H. Rabitz and T. Weinacht, *J. Chem. Phys*., 2005, **122**, 124306.
68 M. Wollenhaupt, A. Präkelt, C. Sarpe-Tudoran, D. Liese and T. Baumert, *J. Opt. B*, 2005, **7**, S270.
69 D. Meshulach and Y. Silberberg, *Phys. Rev. A*, 1999, **60**, 1287.
70 T. C. Weinacht, J. Ahn and P. H. Bucksbaum, *Nature*, 1999, **397**, 233.
71 R. Bartels, S. Backus, E. Zeek, L. Misoguti, G. Vdovin, I. P. Christov, M. M. Murnane and H. C. Kapteyn, *Nature*, 2000, **406**, 164.
72 T. Pfeifer, D. Walter, C. Winterfeldt, C. Spielmann and G. Gerber, *Appl. Phys. B*, 2005, **80**, 277.
73 T. Pfeifer, R. Kemmer, R. Spitzenpfeil, D. Walter, C. Winterfeldt, G. Gerber and C. Spielmann, *Opt. Lett*., 2005, **30**, 1497.
74 T. Pfeifer, C. Spielmann and G. Gerber, *Rep. Prog. Phys*., 2006, **69**, 443.
75 P. Brumer and M. Shapiro, *Annu. Rev. Phys. Chem*., 1992, **43**, 257–282.
76 R. J. Gordon and S. A. Rice, *Annu. Rev. Phys. Chem*., 1997, **48**, 601–641.
77 M. Shapiro and P. Brumer, *J. Chem. Soc., Faraday Trans*., 1997, **93**, 1263.
78 H. Rabitz, R. de Vivie-Riedle, M. Motzkus and K. Kompa, *Science*, 2000, **288**, 824.
79 T. Brixner and G. Gerber, *ChemPhysChem*, 2003, **4**, 418.
80 M. Dantus and V. V. Lozovoy, *Chem. Rev*., 2004, **104**, 1813–1859.
81 M. Wollenhaupt, V. Engel and T. Baumert, *Annu. Rev. Phys. Chem*., 2004, **56**, 25–56.
82 R. E. Carley, E. Heesel and H. H. Fielding, *Chem. Soc. Rev*., 2005, **34**, 949.
83 J. Manz, in *Femtochemistry and Femtobiology*, ed. V. Sundström, Imperial College Press, London, 1996, ch. 3, pp. 80–318.
84 *Advances in Chemical Physics, Volume 101: Chemical Reactions and Their Control on the Femtosecond Time Scale*, ed. P. Gaspard and I. Burghardt, Wiley & Sons, New York, 1997.
85 *Femtochemistry*, ed. F. C. De Schryver, S. De Feyter and G. Schweitzer, Wiley-VCH, Weinheim, 2001.
86 *Laser Control and Manipulation of Molecules*, ed. A. D. Bandrauk, Y. Fujimura and R. J. Gordon, American Chemical Society Publications, Washington DC, 2002, Symposium series, vol. 821.
87 T. Brixner, N. Damrauer and G. Gerber, in *Advances in Atomic, Molecular and Optical Physics*, ed. B. Bederson and H. Walther, Academic Press, San Diego, 2001, vol. 46, pp. 1–54.
88 T. Brixner, T. Pfeifer, G. Gerber, M. Wollenhaupt and T. Baumert, in *Femtosecond Laser Spectroscopy*, ed. P. Hannaford, Springer Science and Business Media, New York, 1st edn, 2004, ch. 9, pp. 225–266.
89 S. A. Rice and M. Zhao, *Optical Control of Molecular Dynamics*, Wiley & Sons, New York, 2000.
90 P. Brumer and M. Shapiro, *Principles of the Quantum Control of Molecular Processes*, Wiley-Interscience, Hoboken NJ, 2003.
91 S. Backus, C. G. Durfee III, M. M. Murnane and H. C. Kapteyn, *Rev. Sci. Instrum*., 1998, **69**, 1207.
92 G. Steinmeyer, *J. Opt. A*, 2003, **5**, R1.
93 U. Keller, *Nature*, 2003, **424**, 831.
94 T. Wilhelm, J. Piel and E. Riedle, *Opt. Lett*., 1997, **22**, 1494.
95 G. Cerullo, M. Nisoli and S. D. Silvestri, *Appl. Phys. Lett*., 1998, **71**, 3616.
96 A. Shirakawa and T. Kobayashi, *Appl. Phys. Lett*., 1998, **72**, 147.
97 C. J. Bardeen, J. Che, K. R. Wilson, V. V. Yakovlev, V. A. Apkarian, C. C. Martens, R. Zadoyan, B. Kohler and M. Messina, *J. Chem. Phys*., 1997, **106**, 8486.
98 M. Gühr, H. Ibrahim and N. Schwentner, *Phys. Chem. Chem. Phys*., 2004, **6**, 5353.
99 M. Fushitani, M. Bargheer, M. Gühr and N. Schwentner, *Phys. Chem. Chem. Phys*., 2005, **7**, 3143.
100 A. Bartana, U. Banin, S. Ruhman and R. Kosloff, *Chem. Phys. Lett*., 1994, **229**, 211.
101 U. Banin, A. Bartana, S. Ruhman and R. Kosloff, *J. Chem. Phys*., 1994, **101**, 8461.
102 E. Gershgoren, J. Vala, R. Kosloff and S. Ruhman, *J. Phys. Chem. A*, 2001, **105**, 5081.
103 D. A. V. Kliner, J. C. Alfano and P. F. Barbara, *J. Chem. Phys*., 1992, **98**, 5375.
104 K. R. Wilson, C. Bardeen, C. P. J. Barty, G. J. Brakenhoff, A. H. Buist, J. Cao, S. D. Carpenter, J. W. Che, D. N. Fittinghoff, M. Müller, J. A. Squier, W. S. Warren, P. M. Weber and V. V. Yakovlev, *Proc. SPIE*, 1998, **3273**, 214.
105 T. Brixner, N. H. Damrauer, P. Niklaus and G. Gerber, *Nature*, 2001, **414**, 57.
106 S.-H. Lee, K.-H. Jung, J.-H. Sung, K.-H. Hong and C. H. Nam, *J. Chem. Phys*., 2006, **117**, 9858.
107 K. A. Walowicz, I. Pastirk, V. V. Lozovoy and M. Dantus, *J. Phys. Chem. A*, 2002, **106**, 9369.
108 T. Brixner, N. H. Damrauer, B. Kiefer and G. Gerber, *J. Chem. Phys*., 2003, **118**, 3692.
109 G. Vogt, G. Krampert, P. Niklaus, P. Nuernberger and G. Gerber, *Phys. Rev. Lett*., 2005, **94**, 068305.
110 V. I. Prokhorenko, A. M. Nagy and R. J. D. Miller, *J. Chem. Phys*., 2005, **122**, 184502.
111 S. Zhang, Z. Sun, X. Zhang, Y. Xu, Z. Wang, Z. Xu and R. Li, *Chem. Phys. Lett*., 2005, **415**, 346.
112 O. Nahmias, O. Bismuth, A. Shoshana and S. Ruhman, *J. Phys. Chem. A*, 2005, **109**, 8246.
113 T. Okada, I. Otake, R. Mizoguchi, K. Onda, S. S. Kano and A. Wada, *J. Chem. Phys*., 2004, **121**, 6386.
114 I. Otake, S. S. Kano and A. Wada, *J. Chem. Phys*., 2006, **124**, 014501.
115 F. Gai, J. Cooper McDonald and P. A. Anfinrud, *J. Am. Chem. Soc*., 1997, **119**, 6201.
116 S. L. Logunov, V. V. Volkov, M. Braun and M. El-Sayed, *Proc. Natl. Acad. Sci. U. S. A*., 2001, **98**, 8475.
117 S. Ruhman, B. Hou, N. Friedman, M. Ottolenghi and M. Sheves, *J. Am. Chem. Soc*., 2002, **124**, 8854.
118 J. L. Herek, W. Wohlleben, R. J. Cogdell, D. Zeidler and M. Motzkus, *Nature*, 2002, **417**, 533.
119 H. Kawano, Y. Nabekawa, A. Suda, Y. Oishi, H. Mizuno, A. Miyawaki and K. Midorikawa, *Biochem. Biophys. Res. Commun*., 2003, **311**, 592.
120 D. S. Larsen, I. H. M. van Stokkum, M. Vengris, M. A. van der Horst, F. L. de Weerd, K. J. Hellingwerf and R. van Grondelle, *Biophys. J*., 2004, **87**, 1858.
121 D. S. Larsen, M. Vengris, I. H. M. van Stokkum, M. A. van der Horst, F. L. de Weerd, K. J. Hellingwerf and R. van Grondelle, *Biophys. J*., 2004, **86**, 2538.
122 D. S. Larsen and R. van Grondelle, *ChemPhysChem*, 2005, **6**, 828.
123 M. Vengris, I. H. M. van Stokkum, X. He, A. F. Bell, P. J. Tonge, R. van Grondelle and D. S. Larsen, *J. Phys. Chem. A*, 2004, **108**, 4587.
124 M. Vengris, D. S. Larsen, M. A. van der Horst, O. F. A. Larsen, K. J. Hellingwerf and R. van Grondelle, *J. Phys. Chem. B*, 2005, **109**, 4197.
125 W. Wohlleben, T. Buckup, J. L. Herek and M. Motzkus, *ChemPhysChem*, 2005, **6**, 850.
126 T. Buckup, T. Lebold, A. Weigel, W. Wohlleben and M. Motzkus, *J. Photochem. Photobiol., A*, 2006, **314**, 314–321.
127 V. I. Prokhorenko, A. M. Nagy, S. A. Waschuk, L. S. Brown, R. R. Birge and R. J. D. Miller, *Science*, 2006, **313**, 1257.
128 G. Vogt, P. Nuernberger, T. Brixner and G. Gerber, *Chem. Phys. Lett*., 2006, **433**, 211.
129 J. P. Ogilvie, D. Débarre, X. Solinas, J.-L. Martin, E. Beaurepaire and M. Joffre, *Opt. Express*, 2006, **14**, 759.
130 M. Shapiro and P. Brumer, *J. Chem. Phys*., 1991, **85**, 8658.
131 A. Salam and J. Meath, *J. Chem. Phys*., 1997, **106**, 7865.
132 Y. Fujimura, L. González, K. Hoki and Y. Ohtsuki, *Chem. Phys. Lett*., 1999, **306**, 1.
133 S. S. Bychkov, B. A. Grishanin and V. N. Zadkov, *J. Exp. Theor. Phys*., 2000, **93**, 24.
134 M. Shapiro and E. Frishman, *Phys. Rev. Lett*., 2000, **84**, 1669.
135 K. Hoki, Y. Ohtsuki and Y. Fujimura, *J. Chem. Phys*., 2001, **114**, 1575.
136 S. S. Bychkov, B. A. Grishanin and V. N. Zadkov, *J. Exp. Theor. Phys*., 2001, **93**, 31.
137 P. Král and M. Shapiro, *Phys. Rev. Lett*., 2001, **87**, 183002.

138 D. Gerbasi, M. Shapiro and P. Brumer, *J. Chem. Phys.*, 2001, **115**, 5349.
139 P. Brumer, E. Frishman and M. Shapiro, *Phys. Rev. A*, 2001, **65**, 015401.
140 Y. Ohta, K. Hoki and Y. Fujimura, *J. Chem. Phys.*, 2002, **116**, 7509.
141 K. Hoki, L. González and Y. Fujimura, *J. Chem. Phys.*, 2002, **116**, 8799.
142 H. Umeda, M. Takagi, S. Yamada, S. Koseki and Y. Fujimura, *J. Am. Chem. Soc.*, 2002, **124**, 9265.
143 P. Král, I. Thanopulos, M. Shapiro and D. Cohen, *Phys. Rev. Lett.*, 2003, **90**, 033001.
144 G. L. J. A. Rikken and E. Raupach, *Nature*, 2000, **405**, 932.
145 W. A. Bonner and B. D. Bean, *Origins Life Evol. Biosphere*, 2000, **30**, 513.
146 M. Motzkus, S. Pedersen and A. H. Zewail, *J. Chem. Phys.*, 1996, **100**, 5620.
147 S. Mukamel, *Principles of Nonlinear Optical Spectroscopy*, Oxford University Press, New York, 1995.
148 D. Jonas, *Annu. Rev. Phys. Chem.*, 2003, **54**, 425.
149 M. C. Asplund, M. T. Zanni and R. M. Hochstrasser, *Proc. Natl. Acad. Sci. U. S. A.*, 2000, **97**, 8219.
150 S. Mukamel, *Annu. Rev. Phys. Chem.*, 2000, **51**, 691.
151 J. C. Wright, *Int. Rev. Phys. Chem.*, 2002, **21**, 185.
152 M. Khalil, N. Demirdöven and A. Tokmakoff, *J. Phys. Chem. A*, 2003, **107**, 5258.
153 J. B. Asbury, *Phys. Rev. Lett.*, 2003, **91**, 237402.
154 V. Cervetto, J. Helbing, J. Bredenbeck and P. Hamm, *J. Chem. Phys.*, 2004, **121**, 5935.
155 T. Brixner, J. Stenger, H. M. Vaswani, M. Cho, R. E. Blankenship and G. R. Fleming, *Nature*, 2005, **434**, 625.
156 T. Frohnmeyer, M. Hofmann, M. Strehle and T. Baumert, *Chem. Phys. Lett.*, 1999, **312**, 447.
157 A. Assion, T. Baumert, U. Weichmann and G. Gerber, *Phys. Rev. Lett.*, 2001, **86**, 5695.
158 H. Niikura, D. M. Villeneuve and P. B. Corkum, *Phys. Rev. Lett.*, 2004, **92**, 133002.
159 C. Trallero-Herrero, J. L. Cohen and T. C. Weinacht, *Phys. Rev. Lett.*, 2006, **96**, 063603.
160 B. J. Sussman, D. Townsend, M. Y. Ivanov and A. Stolow, *Science*, 2006, **314**, 278–281.
161 B. M. Garraway and K.-A. Suominen, *Rep. Prog. Phys.*, 1995, **58**, 365.
162 A. J. Wurzer, W. T. J. Piel and E. Riedle, *Chem. Phys. Lett.*, 1999, **299**, 296.
163 S. L. Dexheimer, Q. Wang, L. A. Peteanu, W. T. Pollard, R. A. Mathies and C. V. Shank, *Chem. Phys. Lett.*, 1992, **188**, 61.
164 C. J. Bardeen, Q. Wang and C. V. Shank, *J. Phys. Chem. A*, 1998, **102**, 2759.
165 H. l. Fragnito, J. Y. Bigot, P. C. Becker and C. V. Shank, *Chem. Phys. Lett.*, 1989, **160**, 101.
166 M. H. Vos and J.-L. Martin, *Biochim. Biophys. Acta*, 1999, **1411**, 1–20.
167 T. Kobayashi, T. Saito and H. Ohtani, *Nature*, 2001, **414**, 531.
168 O. E. Martínez, *IEEE J. Quantum Electron.*, 1988, **24**, 2530–2536.
169 L. Xu, N. Nakagawa, R. Morita, H. Shigekawa and M. Yamashita, *IEEE J. Quantum Electron.*, 2000, **36**, 893.
170 E. Lioudakis, K. Adamou and A. Othonos, *Opt. Eng.*, 2005, **44**, 034203.
171 T. Binhammer, E. Rittweger, R. Ell, F. X. Kärtner and U. Morgner, *IEEE J. Quantum Electron.*, 2005, **41**, 1552.
172 A. M. Weiner, D. E. Leaird, J. S. Patel and J. R. Wullert, *Opt. Lett.*, 1990, **15**, 326.
173 A. M. Weiner, D. E. Leaird, J. S. Patel and J. R. Wullert II, *IEEE J. Quantum Electron.*, 1992, **28**, 908.
174 T. Brixner, G. Krampert, P. Niklaus and G. Gerber, *Appl. Phys. B*, 2002, **74**, S133.
175 T. Brixner, G. Krampert, P. Niklaus and G. Gerber, *J. Opt. Soc. Am. B*, 2003, **20**, 878.
176 T. Brixner, *Appl. Phys. B*, 2003, **76**, 531.
177 T. Suzuki, S. Minemoto and H. Sakai, *Appl. Opt.*, 2004, **43**, 6047.
178 N. Dudovich, D. Oron and Y. Silberberg, *Phys. Rev. Lett.*, 2004, **92**, 103003.
179 T. Suzuki, S. Minemoto, T. Kanai and H. Sakai, *Phys. Rev. Lett.*, 2004, **92**, 133005.
180 T. Brixner, G. Krampert, T. Pfeifer, R. Selle, G. Gerber, M. Wollenhaupt, O. Graefe, C. Horn, D. Liese and T. Baumert, *Phys. Rev. Lett.*, 2004, **92**, 208301.
181 D. Oron, N. Dudovich and Y. Silberberg, *Phys. Rev. Lett.*, 2003, **90**, 213902.
182 Y. Silberberg, *Nature*, 2004, **430**, 624.
183 T. Polack, D. Oron and Y. Silberberg, *Chem. Phys.*, 2005, **318**, 163.
184 L. Polachek, D. Oron and Y. Silberberg, *Opt. Lett.*, 2006, **31**, 631.
185 M. Plewicki, F. Weise, S. M. Weber and A. Lindinger, *Appl. Opt.*, 2006, **45**, 8354.
186 F. Weise, S. M. Weber, M. Plewicki and A. Lindinger, *Chem. Phys.*, 2007, **332**, 313.
187 M. Aeschlimann, M. Bauer, D. Bayer, T. Brixner, F. J. García de Abajo, W. Pfeiffer, M. Rohmer, C. Spindler and F. Steeb, *Nature*, 2007, **446**, 301.
188 Y. Kobayashi, Y. Igasaki, N. Yoshida, N. Fukuchi, H. Toyoda, T. Hara and M. H. Wu, *Proc. SPIE*, 2000, **3951**, 158.
189 T. Feurer, J. C. Vaughan, R. M. Koehl and K. A. Nelson, *Opt. Lett.*, 2002, **27**, 652.
190 J. C. Vaughan, T. Feurer and K. A. Nelson, *J. Opt. Soc. Am. B*, 2002, **19**, 2489.
191 D. Walter, T. Pfeifer, C. Winterfeldt, R. Kemmer, R. Spitzenpfeil, G. Gerber and C. Spielmann, *Opt. Express*, 2006, **14**, 3433.
192 T. Pfeifer, L. Gallmann, M. J. Abel, D. M. Neumark and S. R. Leone, *Opt. Lett.*, 2006, **31**, 2326.
193 H. Itoh, T. Urakami, S. Aoshima and Y. Tsuchiya, *Jpn. J. Appl. Phys.*, 2006, **45**, 5761–5763.
194 M. A. Dugan, J. X. Tull and W. S. Warren, *J. Opt. Soc. Am. B.*, 1997, **14**(9), 2348–2358.
195 E. Z. K. Maginnis, S. Backus, U. Russek, M. Murnane, G. Mourou and H. Kapteyn, *Opt. Lett.*, 1999, **24**, 493.
196 A. Baltuška and T. Kobayashi, *Appl. Phys. B*, 2002, **75**, 427.
197 C. Radzewicz, P. Wasylczyk, W. Wasukewsju and J. S. Krasiński, *Opt. Lett.*, 2004, **29**, 177–179.
198 K. Li, U. Krishnamorthy, J. P. Heritage and O. Solgaard, *Opt. Lett.*, 2002, **27**, 366–368.
199 M. Hacker, G. Stobrawa, R. Sauerbrey, T. Buckup, M. Motzkus, M. Wildenhain and A. Gehner, *Appl. Phys. B*, 2003, **76**, 711–714.
200 A. Suda, Y. Oishi, K. Nagasaka, P. Wang and K. Midorikawa, *Opt. Express*, 2001, **9**, 2–6.
201 Y. Oishi, A. Suda, F. Kannari and K. Midorikawa, *Opt. Commun.*, 2007, **270**, 305–309.
202 F. Verluise, V. Laude, Z. Cheng, C. Spielmann and P. Tournois, *Opt. Lett.*, 2000, **25**, 575.
203 M. Roth, M. Mehendale, A. Bartelt and H. Rabitz, *Appl. Phys. B*, 2005, **80**, 441–444.
204 Y. Huang and A. Dogariu, *Opt. Express*, 2006, **14**, 10089.
205 F. Eickemeyer, R. A. Kaindl, M. Woerner, T. Elsaesser and A. M. Weiner, *Opt. Lett.*, 2000, **25**, 1472.
206 N. Belabas, J.-P. Likforman, L. Canioni, B. Bousquet and M. Joffre, *Opt. Lett.*, 2001, **26**, 743.
207 T. Witte, D. Zeidler, D. Proch, K. L. Kompa and M. Motzkus, *Opt. Lett.*, 2002, **27**, 131.
208 H.-S. Tan, E. Schreiber and W. S. Warren, *Opt. Lett.*, 2002, **27**, 439.
209 H.-S. Tan and W. S. Warren, *Opt. Express*, 2003, **11**, 1021.
210 T. Witte, K. L. Kompa and M. Motzkus, *Appl. Phys. B*, 2003, **76**, 467.
211 N. A. Naz, H. S. S. Hung, M. V. O'Connor, D. C. Hanna and D. P. Shepherd, *Opt. Express*, 2005, **13**, 8400.
212 S.-H. Shim, D. B. Strasfeld, E. C. Fulmer and M. T. Zanni, *Opt. Lett.*, 2006, **31**, 838.
213 M. Hacker, R. Netz, M. Roth, G. Stobrawa, T. Feurer and R. Sauerbrey, *Appl. Phys. B*, 2001, **73**, 273–277.
214 M. Hacker, T. Feurer, R. Sauerbrey, T. Lucza and G. Szabo, *J. Opt. Soc. Am. B*, 2001, **18**, 866–871.
215 H. Wang and A. M. Weiner, *IEEE J. Quantum Electron.*, 2004, **40**, 937–945.
216 C. Schriever, S. Lochbrunner, M. Optiz and E. Riedle, *Opt. Lett.*, 2006, **31**, 543–545.
217 P. Nuernberger, G. Vogt, R. Selle, S. Fechner, T. Brixner and G. Gerber, *Proc. SPIE*, 2006, **6187**, 61870M.
218 E. Åkesson, H. Bergström, V. Sundström and T. Gillbro, *Chem. Phys. Lett.*, 1986, **126**, 385.

219 T. Kühne, R. Küster and P. Vöhringer, *Chem. Phys.*, 1998, **233**, 161.
220 P. H. Bucksbaum, *Nature*, 1998, **396**, 217.
221 L. Nikowa, D. Schwarzer and J. Troe, *Chem. Phys. Lett.*, 1995, **233**, 303.
222 S. A. Kovalenko, J. Ruthmann and N. P. Ernsting, *J. Chem. Phys.*, 1998, **109**, 1894.
223 P. Changenet-Barret, C. T. Choma, E. F. Gooding, W. F. Degrado and R. M. Hochstrasser, *J. Phys. Chem. B*, 2000, **104**, 9322.
224 D. F. Larsen, E. Papagiannakis, I. H. M. van Stokkum, M. Vengris, J. T. M. Kennis and R. van Grondelle, *Chem. Phys. Lett.*, 2003, **381**, 733.
225 K. M. Gaab and C. J. Bardeen, *J. Phys. Chem. A*, 2004, **108**, 10801.
226 R. H. Sension, S. T. Repinec, A. Z. Szarka and R. M. Hochstrasser, *J. Chem. Phys.*, 1992, **98**, 6291.
227 C. J. Bardeen, Q. Wang and C. V. Shank, *Phys. Rev. Lett.*, 1995, **75**, 3410.
228 G. Cerullo, C. J. Bardeen, Q. Wang and C. V. Shank, *Chem. Phys. Lett.*, 1996, **262**, 362.
229 V. D. Kleiman, S. M. Arrivo, J. S. Melinger and E. J. Heilweil, *Chem. Phys.*, 1998, **233**, 207.
230 C. J. Bardeen, V. V. Yakovlev, J. A. Squier and K. R. Wilson, *J. Am. Chem. Soc.*, 1998, **120**, 13023.
231 G. J. Brakenhoff, A. H. Buist, M. Müller, J. A. Squier, C. J. Bardeen, V. V. Yakovlev and K. R. Wilson, *Proc. SPIE*, 1999, **3605**, 40.
232 K. Misawa and T. Kobayashi, *J. Chem. Phys.*, 2000, **113**, 7546.
233 T. Chen, A. Vierheilig, P. Waltner, M. Heid, W. Kiefer and A. Materny, *Chem. Phys. Lett.*, 2000, **326**, 375.
234 T. Hellerer, A. M. K. Enejder and A. Zumbusch, *Appl. Phys. Lett.*, 2004, **85**, 25.
235 K. P. Knutsen, J. C. Johnson, A. E. Miller, P. B. Petersen and R. J. Saykally, *Chem. Phys. Lett.*, 2004, **387**, 436.
236 S. Malkmus, R. Dürr, C. Sobotta, H. Pulvermacher, W. Zinth and M. Braun, *J. Phys. Chem. A*, 2005, **109**, 10488.
237 G. Vogt, P. Nuernberger, R. Selle, F. Dimler, T. Brixner and G. Gerber, *Phys. Rev. A*, 2006, **74**, 033413.
238 S. M. Arrivo, T. P. Dougherty, W. T. Grubbs and E. J. Heilweil, *Chem. Phys. Lett.*, 1995, **235**, 247.
239 T. Witte, T. Hornung, L. Windhorn, D. Proch, R. de Vivie-Riedle and M. Motzkus, *J. Chem. Phys.*, 2003, **118**, 2021.
240 T. Witte, J. S. Yeston, M. Motzkus, E. J. Heilweil and K. L. Kompa, *Chem. Phys. Lett.*, 2004, **392**, 156.
241 V. V. Lozovoy, I. Pastirk, K. A. Walowicz and M. Dantus, *J. Chem. Phys.*, 2003, **118**, 3187.
242 I. Pastirk, J. M. Dela Cruz, K. A. Walowicz, V. V. Lozovoy and M. Dantus, *Opt. Express*, 2003, **11**, 1695.
243 J. Chen, H. Kawano, Y. Nabekawa, H. Mizuno, A. Miyawaki, T. Tanabe, F. Kannari and K. Midorikawa, *Opt. Express*, 2004, **15**, 3408.
244 T. Brixner, G. Krampert, P. Niklaus and G. Gerber, *J. Mod. Opt.*, 2003, **50**, 539.
245 J. M. Dela Cruz, I. Pastirk, V. V. Lozovoy, K. A. Walowicz and M. Dantus, *J. Phys. Chem. A*, 2004, **108**, 53.
246 J. M. Dela Cruz, I. Pastirk, M. Comstock and M. Dantus, *Opt. Express*, 2004, **12**, 4144.
247 J. M. Dela Cruz, I. Pastirk, M. Comstock, V. V. Lozovoy and M. Dantus, *Proc. Natl. Acad. Sci. U. S. A.*, 2004, **101**, 16996.
248 K. J. Kubarych, J. P. Ogilvie, A. Alexandrou and M. Joffre, *Ultrafast Phenomena XIV: Springer Series in Chemical Physics*, 2004, **79**, 575.
249 J. P. Ogilvie, K. J. Kubarych, A. Alexandrou and M. Joffre, *Opt. Lett.*, 2005, **30**, 911.
250 J. Dela Cruz, V. V. Lozovoy and M. Dantus, *J. Photochem. Photobiol., A*, 2006, **180**, 307–313.
251 A. M. Weiner, D. E. Leaird, G. P. Wiederrecht and K. A. Nelson, *Science*, 1990, **247**, 1317.
252 J. Ventalon, J. M. Fraser, M. H. Vos, A. Alexandrou, J.-L. Martin and M. Joffre, *Proc. Natl. Acad. Sci. U. S. A.*, 2004, **101**, 13216.
253 A. M. Weiner, D. E. Leaird, G. P. Wiederrecht and K. A. Nelson, *J. Opt. Soc. Am. B*, 1991, **8**, 1264.
254 A. M. Weiner, *Prog. Quant. Electron.*, 1995, **19**, 161.
255 T. C. Weinacht, J. L. White and P. H. Bucksbaum, *J. Phys. Chem. A*, 1999, **103**, 10166.
256 M. Spanner and P. Brumer, *Phys. Rev. A*, 2006, **73**, 023809.
257 M. Spanner and P. Brumer, *Phys. Rev. A*, 2006, **73**, 023810.
258 J. Konradi, A. K. Singh and A. Materny, *Phys. Chem. Chem. Phys.*, 2005, **7**, 3574.
259 D. Oron, N. Dudovich, D. Yelin and Y. Silberberg, *Phys. Rev. A*, 2002, **65**, 043408.
260 D. Oron, N. Dudovich, D. Yelin and Y. Silberberg, *Phys. Rev. Lett.*, 2002, **88**, 063004.
261 D. Zeidler, S. Frey, W. Wohlleben, M. Motzkus, F. Busch, T. Chen, W. Kiefer and A. Materny, *J. Chem. Phys.*, 2002, **116**, 5231.
262 J. Konradi, A. K. Singh and A. Materny, *J. Photochem. Photobiol., A*, 2006, **180**, 289–299.
263 J. Konradi, A. K. Singh, A. V. Scaria and A. Materny, *J. Raman Spectrosc.*, 2006, **37**, 697–704.
264 N. Dudovich, D. Oron and Y. Silberberg, *Nature*, 2002, **418**, 512.
265 D. Oron, N. Dudovich and Y. Silberberg, *Phys. Rev. Lett.*, 2002, **89**, 273001.
266 N. Dudovich, D. Oron and Y. Silberberg, *J. Chem. Phys.*, 2003, **118**, 9208.
267 B. von Vacano, W. Wohlleben and M. Motzkus, *Opt. Lett.*, 2006, **31**, 413.
268 B. von Vacano, W. Wohlleben and M. Motzkus, *J. Raman Spectrosc.*, 2006, **37**, 404.
269 B. von Vacano and M. Motzkus, *Opt. Commun.*, 2006, **264**, 488–493.
270 K. Itoh, Y. Toda, R. Morita and M. Yamashita, *Jpn. J. Appl. Phys.*, 2004, **43**, 6448.
271 P. Nuernberger, G. Vogt, G. Gerber, R. Improta and F. Santoro, *J. Chem. Phys.*, 2006, **125**, 044512.
272 G. Vogt, P. Nuernberger, G. Gerber, R. Improta and F. Santoro, *J. Chem. Phys.*, 2006, **125**, 044513.
273 K. Hoki and P. Brumer, *Phys. Rev. Lett.*, 2005, **95**, 168305.
274 R. Improta and F. Santoro, *J. Chem. Theory Comput.*, 2005, **1**, 215.
275 A. Sanchez-Galvez, P. Hunt, M. A. Robb, M. Olivucci, T. Vreven and H. Schlegel, *J. Am. Chem. Soc.*, 2000, **122**, 2911.
276 F. Großmann, L. Feng, G. Schmidt, T. Kunert and R. Schmidt, *Europhys. Lett.*, 2002, **60**, 201.
277 P. A. Hunt and M. A. Robb, *J. Am. Chem. Soc.*, 2005, **127**, 5720.
278 B. Dietzek, B. Brüggemann, T. Pascher and A. Yartsev, *Phys. Rev. Lett.*, 2006, **97**, 258301.
279 W. Jakubetz and B. L. Lan, *Chem. Phys.*, 1997, **217**, 375.
280 S. P. Shah and S. A. Rice, *Faraday Discuss.*, 1999, **113**, 319.
281 S. P. Shah and S. A. Rice, *J. Chem. Phys.*, 2000, **113**, 6536.
282 V. Kurkal and S. A. Rice, *Chem. Phys. Lett.*, 2001, **344**, 125.
283 C. Uiberacker and W. Jakubetz, *J. Chem. Phys.*, 2004, **120**, 11532.
284 C. Uiberacker and W. Jakubetz, *J. Chem. Phys.*, 2004, **120**, 11540.
285 J. Gong, A. Ma and S. A. Rice, *J. Chem. Phys.*, 2005, **122**, 144311.
286 J. Gong, A. Ma and S. A. Rice, *J. Chem. Phys.*, 2005, **122**, 204505.
287 S. C. Flores and V. S. Batista, *J. Phys. Chem. B*, 2004, **108**, 6745–6749.
288 M. Abe, Y. Ohtsuki, Y. Fujimura and W. Domcke, *J. Chem. Phys.*, 2005, **123**, 144508.
289 Y. Ohtsuki, K. Ohara, M. Abe, K. Nakagami and Y. Fujimura, *Chem. Phys. Lett.*, 2003, **369**, 525.
290 P. Marquetand, P. Nuernberger, G. Vogt, T. Brixner, V. Engel and G. Gerber, *Characteristics of wave packet evolution from quantum control landscapes*, in preparation.
291 B. V. O'Grady and R. J. Donovan, *Chem. Phys. Lett.*, 1985, **122**, 503.
292 N. F. Scherer, L. R. Khundkar, R. B. Bernstein and A. H. Zewail, *J. Chem. Phys.*, 1987, **87**, 1451.
293 C. Wittig, S. Sharpe and R. A. Beaudet, *Acc. Chem. Res.*, 1988, **21**, 341.
294 N. F. Scherer, C. Sipes, R. B. Bernstein and A. H. Zewail, *J. Chem. Phys.*, 1990, **92**, 5239.
295 S. I. Ionov, G. A. Brucker, C. Jaques, L. Valachovic and C. Wittig, *J. Chem. Phys.*, 1993, **99**, 6553.

296 U. Marvet and M. Dantus, *Chem. Phys. Lett*., 1995, **245**, 393.
297 V. A. Apkarian, *J. Chem. Phys*., 1996, **106**, 5298.
298 P. Gross and M. Dantus, *J. Chem. Phys*., 1997, **106**, 8013.
299 P. Backhaus and B. Schmidt, *Chem. Phys*., 1997, **217**, 131.
300 J. D. Simon and X. Xie, *J. Phys. Chem*., 1986, **90**, 6751.
301 J. D. Simon and X. Xie, *J. Phys. Chem*., 1987, **91**, 5538.
302 R. Zadoyan and V. A. Apkarian, *Chem. Phys. Lett*., 1993, **206**, 475.
303 T. Lian, S. E. Bromberg, M. C. Asplund, H. Yang and C. B. Harris, *J. Phys. Chem*., 1996, **100**, 11994.
304 H. Yang, K. T. Kotz, M. Aplund and C. B. Harris, *J. Am. Chem. Soc*., 1997, **119**, 9564.
305 J. B. Asbury, H. N. Gosh, J. S. Yeston, R. G. Bergman and T. Lian, *Organometallics*, 1998, **17**, 3417.
306 H. Yang, P. T. Snee, K. T. Kotz, C. K. Payne, H. Frei and C. B. Harris, *J. Am. Chem. Soc*., 1999, **121**, 9227.
307 P. T. Snee, A. Yang, K. T. Kotz, C. K. Payne and C. B. Harris, *J. Phys. Chem. A*, 1999, **103**, 10426.
308 P. T. Snee, C. K. Payne, S. D. Mebane, K. T. Kotz and C. B. Harris, *J. Am. Chem. Soc*., 2001, **123**, 6909.
309 P. T. Snee, K. Payne, K. T. Kotz, H. Yang and C. B. Harris, *J. Am. Chem. Soc*., 2001, **123**, 2255.
310 M. C. Asplund, P. T. Snee, J. S. Yeston, M. J. Wilkens, C. K. Payne, H. Yang, K. T. Kotz, H. Frei, R. G. Bergman and C. B. Harris, *J. Am. Chem. Soc*., 2002, **124**, 10605.
311 B. A. Arndtsen, R. G. Bergman, T. A. Mobley and T. H. Peterson, *Acc. Chem. Res*., 1995, **28**, 28.
312 P. Brumer, A. Abrashkevich and M. Shapiro, *Faraday Discuss*., 1999, **113**, 291.
313 K. M. Jones, E. Tiesinga, P. D. Lett and P. S. Julienne, *Rev. Mod. Phys*., 2006, **78**, 483.
314 C. P. Koch, J. P. Palao, R. Kosloff and F. Masnou-Seeuws, *Phys. Rev. A*, 2004, **70**, 013402.
315 E. Luc-Koenig, R. Kosloff, F. Masnou-Seeuws and M. Vatasescu, *Phys. Rev. A*, 2004, **70**, 033414.
316 E. Luc-Koenig, M. Vatasescu and F. Masnou-Seeuws, *Eur. Phys. J. D*, 2004, **31**, 239.
317 C. P. Koch, E. Luc-Koenig and F. Masnou-Seeuws, *Phys. Rev. A*, 2006, **73**, 033408.
318 W. Salzmann, U. Poschinger, R. Wester, M. Weidemüller, A. Merli, S. M. Weber, F. Sauer, M. Plewicki, F. Weise, A. M. Esparza, L. Wöste and A. Lindinger, *Phys. Rev. A*., 2006, **73**, 023414.
319 B. L. Brown, A. J. Dicks and I. A. Walmsley, *Phys. Rev. Lett*., 2006, **96**, 173002.
320 B. L. Brown, A. J. Dicks and I. A. Walmsley, *Opt. Commun*., 2006, **264**, 278.
321 B. L. Feringa, *Molecular Switches*, Wiley-VCH, Weinheim, 2001.
322 H. Abramczyk, *J. Chem. Phys*., 2004, **120**, 11120.
323 C. R. Mendonça, U. M. Neves, I. Guedes, S. C. Zilio and L. Misoguti, *Phys. Rev. A*, 2006, **74**, 025401.